



HAL
open science

Mathematical analysis of a three-tiered model of anaerobic digestion

Sarra Nouaoura, Nahla Abdellatif, Radhouane Fekih-Salem, Tewfik Sari

► **To cite this version:**

Sarra Nouaoura, Nahla Abdellatif, Radhouane Fekih-Salem, Tewfik Sari. Mathematical analysis of a three-tiered model of anaerobic digestion. *SIAM Journal on Applied Mathematics*, 2021, 81 ((3)), pp.1264-1286. 10.1137/20M1353897 . hal-02540350v3

HAL Id: hal-02540350

<https://hal.science/hal-02540350v3>

Submitted on 12 Jan 2021

HAL is a multi-disciplinary open access archive for the deposit and dissemination of scientific research documents, whether they are published or not. The documents may come from teaching and research institutions in France or abroad, or from public or private research centers.

L'archive ouverte pluridisciplinaire **HAL**, est destinée au dépôt et à la diffusion de documents scientifiques de niveau recherche, publiés ou non, émanant des établissements d'enseignement et de recherche français ou étrangers, des laboratoires publics ou privés.

1 **MATHEMATICAL ANALYSIS OF A THREE-TIERED MODEL OF**
2 **ANAEROBIC DIGESTION ***

3 SARRA NOUAOURA[†], NAHLA ABDELLATIF[‡], RADHOUANE FEKIH-SALEM[§], AND
4 TEWFIK SARI[¶]

5 **Abstract.** In this paper, we are interested in a mechanistic model describing the anaerobic
6 mineralization of chlorophenol in a three-step food-web. The model is a six-dimensional system of
7 ordinary differential equations. In our study, we take into account the phenol and the hydrogen input
8 concentrations as well as the maintenance terms. Moreover, we consider the case of a large class of
9 growth rates, instead of specific kinetics. In this general case, a recent study shows that the system
10 can have up to eight steady states and their existence conditions were analytically determined. We
11 focus here on the necessary and sufficient conditions of the local stability of the steady states, accord-
12 ing to the four operating parameters of the process, which are the dilution rate and the chlorophenol,
13 phenol and hydrogen input concentrations. In previous studies, this stability analysis was performed
14 only numerically. Using the Liénard-Chipart stability criterion, we show that the positive steady
15 state can be unstable and we give numerical evidence for a supercritical Hopf bifurcation with the
16 appearance of a stable periodic orbit. We give two bifurcation diagrams with respect to the dilution
17 rate, first, and then to the chlorophenol input concentration as the bifurcating parameters, showing
18 that the system can present rich behavior including bistability, coexistence and occurrence of limit
19 cycle.

20 **Key words.** Anaerobic digestion, Chemostat, Chlorophenol mineralization, Hopf bifurcation,
21 Liénard-Chipart stability criterion, Limit cycle.

22 **AMS subject classifications.** 34A34, 34D20, 37N25, 92B05

23 **1. Introduction.** Anaerobic digestion is a natural process in which organic ma-
24 terial is converted into biogas in an environment without oxygen by the action of a
25 microbial ecosystem. It is used for the treatment of wastewater and organic solid
26 wastes and has the advantage of producing methane and hydrogen under appropriate
27 conditions [13]. The removed carbon dioxide can be used too as a carbon source
28 for microalgae [12]. It is used also for several industrial or domestic purposes in
29 biorefineries and other anaerobic technologies. For a recent review on the current
30 state-of-the-art with respect to the theory, applications, and technologies, the reader
31 is referred to Wade [25].

32 The full Anaerobic Digestion Model No.1.(ADM1) [1] is highly parameterized with
33 a large number of state variables. Whilst suitable for dynamic simulation, analytical
34 results on the model are impossible and only numerical investigations are available
35 [4]. Due to the analytical intractability of the full ADM1, simpler mechanistic models
36 of microbial interaction have been proposed in view of a better understanding of the
37 anaerobic digestion process.

38 The two-tiered models, which take the form of four-dimensional mathematical
39 models with a cascade of two biological reactions, where one substrate is consumed

*Submitted to the editors 2020-07-17.

Funding: This work was supported by the Euro-Mediterranean research network TREASURE
(<http://www.inra.fr/treasure>).

[†]University of Tunis El Manar, National Engineering School of Tunis, LAMSIN, 1002, Tunis,
Tunisia (sarra.nouaoura@enit.utm.tn).

[‡]University of Manouba, National School of Computer Science, 2010, Manouba, Tunisia
(nahla.abdellatif@ensi-uma.tn).

[§]University of Monastir, Higher Institute of Computer Science of Mahdia, 5111, Mahdia, Tunisia
(radhouene.fekihsaleem@isima.rnu.tn).

[¶]ITAP, Univ Montpellier, INRAE, Institut Agro, Montpellier, France (tewfik.sari@inrae.fr).

40 by one microorganism in a chemostat to produce a product that serves as the main lim-
 41 iting substrate for a second microorganism, are the simplest models which encapsulate
 42 the essence of the anaerobic digestion process. Two-tiered models with commensal-
 43 istic relationship including or not substrate inhibition of the second population are
 44 widely considered [2, 3, 17, 21] where the second population (the commensal popula-
 45 tion) benefits for its growth from the first population (the host population) while the
 46 host population is not affected by the growth of the commensal population. On the
 47 contrary, when the growth of the first population is affected by the growth of the sec-
 48 ond population, the system describes a syntrophic relationship [5, 7, 9, 18, 19, 24, 29].
 49 For more details and informations on commensalism and syntrophy, the reader is
 50 referred to [19] and the references therein. Important and interesting extensions of
 51 the two-tiered models are the eight-dimensional mathematical models, which include
 52 syntrophy and inhibition [27, 28] and the model with five state variables studied in
 53 [4, 15].

54 In this paper, we consider a six-dimensional mathematical model, which is an
 55 extension, with generalized growth functions, of the three-tiered food-web studied by
 56 Wade et al. [26]. For a description of this food-web, where the microorganisms in-
 57 volved are chlorophenol and phenol degraders and hydrogenotrophic methanogen, see
 58 section 4. Note that the three-tiered food-web is not a classical anaerobic digestion
 59 process since the chlorophenol mineralization may occur under aerobic or anaerobic
 60 conditions with different microbial consortia involved. For more details on the biolog-
 61 ical significance of this food-web and its relation to the complete ADM1, the reader
 62 is invited to refer to [26]. It has been shown in [26] that this model can have up to
 63 eight steady states. Arguing that the Routh–Hurwitz theorem allowing for an explicit
 64 analysis of the stability of steady states, is intractable beyond five dimensions, as it
 65 was noticed in [14], the stability of the steady states were determined only numeri-
 66 cally [26] using specific growth rates (see formulas (4.1)). Several operating diagrams,
 67 which are the bifurcation diagrams with respect to the four operating parameters (i.e.
 68 the dilution rate, the chlorophenol, the phenol and the hydrogen input concentrations)
 69 have been numerically constructed in [26], showing the role, and the importance of
 70 each operating parameter, in particular for the coexistence of all three species.

71 The model of [26] is extended in [16, 20] with general growth rates (see section 2
 72 for the assumptions on the growth rates) and takes the form:

$$\begin{aligned}
 & \left\{ \begin{array}{l}
 \dot{x}_0 = (\mu_0(s_0, s_2) - D - a_0)x_0 \\
 \dot{x}_1 = (\mu_1(s_1, s_2) - D - a_1)x_1 \\
 \dot{x}_2 = (\mu_2(s_2) - D - a_2)x_2 \\
 \dot{s}_0 = D(s_0^{\text{in}} - s_0) - \mu_0(s_0, s_2)x_0 \\
 \dot{s}_1 = D(s_1^{\text{in}} - s_1) + \mu_0(s_0, s_2)x_0 - \mu_1(s_1, s_2)x_1 \\
 \dot{s}_2 = D(s_2^{\text{in}} - s_2) - \omega\mu_0(s_0, s_2)x_0 + \mu_1(s_1, s_2)x_1 - \mu_2(s_2)x_2
 \end{array} \right.
 \end{aligned}
 \tag{1.1}$$

75 where s_0 , s_1 and s_2 are the substrate concentrations (chlorophenol, phenol and hy-
 76 drogen, in the application); x_0 , x_1 and x_2 are the biomass concentrations; D is the
 77 dilution rate; μ_i is the specific growth rate; s_i^{in} is the input substrate concentration
 78 in the chemostat; ω is a yield coefficient; a_i is the maintenance (or decay) rate for
 79 $i = 0, 1, 2$ and corresponding to chlorophenol, phenol and hydrogen, respectively. As
 80 explained in [26], the chlorophenol degrader grows on both chlorophenol and hydrogen
 81 and produces phenol. The phenol degrader consumes the phenol to form hydrogen,
 82 which inhibits its growth. The hydrogenotrophic methanogen grows on the produced
 83 hydrogen.

84 The mathematical analysis of (1.1), under various assumptions, is given in [8, 16,
 85 20, 23]. The system (1.1) was studied in [20] in the case $s_0^{\text{in}} > 0$ and $s_1^{\text{in}} = s_2^{\text{in}} = 0$
 86 where at most three types of steady states can exist. The necessary and sufficient
 87 conditions of existence of the steady states are analytically determined, showing their
 88 uniqueness, except for one of them, that can exist in two forms. When maintenance
 89 is neglected (a_0, a_1 and a_2 are assumed to be zero), the six-dimensional mathematical
 90 model can be reduced to a three-dimensional one and the stability of steady states
 91 was analytically characterized. It has been also shown in [20] that the positive steady
 92 state can be unstable, a fact that has not been described in [26]. Numerical analysis
 93 has suggested the presence of a Hopf bifurcation emerging through the positive steady
 94 state, with the chlorophenol input concentration as the bifurcating parameter. System
 95 (1.1) was studied in [23] in the case without maintenance and persistence results were
 96 analytically proved. Using numerical estimation, it is shown in [23] that the system
 97 has a rich dynamics including Hopf, Bogdanov-Takens and Bautin bifurcations. The
 98 three-tiered model of [26] was simplified in [8] by neglecting the part of hydrogen
 99 produced by the phenol degrader ($\mu_1(s_1, s_2)x_1$ is not considered in the model) as well
 100 as maintenance, which gives rise to a less realistic model. However, the existence and
 101 stability of steady states were analytically studied and a global analysis is performed,
 102 proving the asymptotic persistence of the three bacteria. The results of [20] were
 103 extended in [16] in the case $s_1^{\text{in}} \geq 0$ and $s_2^{\text{in}} \geq 0$. When the inflow of the three
 104 substrates is included, the system can have at most eight types of steady states. The
 105 necessary and sufficient conditions of existence of the steady states are analytically
 106 determined when maintenance is included. The necessary and sufficient conditions of
 107 stability are analytically determined only when maintenance is neglected.

108 Here, we focus on the analysis of the stability of all steady states of (1.1), and we
 109 analytically characterize the stability, by using the Liénard-Chipart stability criterion,
 110 in the case including maintenance, where the system cannot be reduced to a three-
 111 dimensional one. We then generalize [26] by allowing a larger class of growth functions
 112 and by giving rigorous proofs for the results on the existence and stability of steady
 113 states. For this class of growth functions, we generalize [8, 16, 20, 23] by giving the
 114 necessary and sufficient conditions of stability of steady states when maintenance is
 115 included in the model.

116 This paper is organized as follows: in [section 2](#), we recall the general assumptions
 117 on the growth functions and the steady states of model (1.1). We give in [section 3](#)
 118 the necessary and sufficient conditions of existence and stability of the steady states.
 119 Next, in [section 4](#), we give an application of our theoretical results to the three-
 120 tiered model considered in [26]. We dedicate [section 5](#) to discuss our results. In
 121 [Appendix A](#), we define some auxiliary functions used for the description of the steady
 122 states with their conditions of existence and stability. The Liénard-Chipart stability
 123 criterion and all the proofs are reported in [Appendices B and C](#), respectively. In
 124 [Appendix D](#), the description of the bifurcation diagram according to the dilution rate
 125 is supported by numerical experimentation. The bifurcation diagram according to the
 126 chlorophenol input concentration is determined in [Appendix E](#) and it is supported by
 127 numerical experimentation in [Appendix F](#). Details and complements on the three-
 128 tiered model considered in [26] are given in [Appendix G](#). In [Appendix H](#), we illustrate
 129 some numerical simulations and some tables are given in [Appendix I](#).

130 **2. Assumptions and steady states.** We consider model (1.1). Following [16,
 131 20], we assume that the growth functions are continuously differentiable (\mathcal{C}^1) and
 132 satisfy the following conditions:

(H1) For all $s_0 > 0$ and $s_2 > 0$, $0 < \mu_0(s_0, s_2) < +\infty$, $\mu_0(0, s_2) = 0$, $\mu_0(s_0, 0) = 0$.

(H2) For all $s_1 > 0$ and $s_2 \geq 0$, $0 < \mu_1(s_1, s_2) < +\infty$, $\mu_1(0, s_2) = 0$.

(H3) For all $s_2 > 0$, $0 < \mu_2(s_2) < +\infty$, $\mu_2(0) = 0$.

(H4) For all $s_0 > 0$ and $s_2 > 0$, $\frac{\partial \mu_0}{\partial s_0}(s_0, s_2) > 0$, $\frac{\partial \mu_0}{\partial s_2}(s_0, s_2) > 0$.

(H5) For all $s_1 > 0$ and $s_2 > 0$, $\frac{\partial \mu_1}{\partial s_1}(s_1, s_2) > 0$, $\frac{\partial \mu_1}{\partial s_2}(s_1, s_2) < 0$.

(H6) For all $s_2 > 0$, $\mu_2'(s_2) > 0$.

(H7) The function $s_2 \mapsto \mu_0(+\infty, s_2)$ is monotonically increasing and the function $s_2 \mapsto \mu_1(+\infty, s_2)$ is monotonically decreasing.

Let Ψ the function defined in Table 8 of Appendix A. Then, we assume that:

(H8) When $\omega < 1$, the function Ψ has a unique minimum $\bar{s}_2 = \bar{s}_2(D)$ on the interval (s_2^0, s_2^1) , such that $\frac{\partial \Psi}{\partial s_2}(s_2, D) < 0$ on (s_2^0, \bar{s}_2) and $\frac{\partial \Psi}{\partial s_2}(s_2, D) > 0$ on (\bar{s}_2, s_2^1) .

All other auxiliary functions needed in the afterward results are provided in Appendix A. Under Hypotheses (H1) to (H6), system (1.1) can have at most eight types of steady states whose components are given in Table 1, see Theorem 1 in [16]. Notice that a steady state exists or is said to be 'meaningful' if and only if all its components are nonnegative.

TABLE 1
Steady states of (1.1). All functions are defined in Table 8.

	s_0, s_1, s_2 and x_0, x_1, x_2 components
SS1	$s_0 = s_0^{\text{in}}, s_1 = s_1^{\text{in}}, s_2 = s_2^{\text{in}}$ and $x_0 = 0, x_1 = 0, x_2 = 0$
SS2	$s_0 = s_0^{\text{in}}, s_1 = s_1^{\text{in}}, s_2 = M_2(D + a_2)$ and $x_0 = 0, x_1 = 0, x_2 = \frac{D}{D+a_2}(s_2^{\text{in}} - s_2)$
SS3	$s_1 = s_1^{\text{in}} + s_0^{\text{in}} - s_0$ and $s_2 = s_2^{\text{in}} - \omega(s_0^{\text{in}} - s_0)$, where s_0 is a solution of $\psi_0(s_0) = D + a_0$ and $x_0 = \frac{D}{D+a_0}(s_0^{\text{in}} - s_0), x_1 = 0, x_2 = 0$
SS4	$s_0 = M_0(D + a_0, s_2)$ and $s_1 = M_1(D + a_1, s_2)$, where s_2 is a solution of $\Psi(s_2, D) = (1 - \omega)s_0^{\text{in}} + s_1^{\text{in}} + s_2^{\text{in}}$ and $x_0 = \frac{D}{D+a_0}(s_0^{\text{in}} - s_0), x_1 = \frac{D}{D+a_1}(s_0^{\text{in}} - s_0 + s_1^{\text{in}} - s_1), x_2 = 0$
SS5	$s_0 = \varphi_0(D), s_1 = s_1^{\text{in}} + s_0^{\text{in}} - s_0, s_2 = M_2(D + a_2)$ and $x_0 = \frac{D}{D+a_0}(s_0^{\text{in}} - s_0), x_1 = 0, x_2 = \frac{D}{D+a_2}(s_2^{\text{in}} - s_2 - \omega(s_0^{\text{in}} - s_0))$
SS6	$s_0 = \varphi_0(D), s_1 = \varphi_1(D), s_2 = M_2(D + a_2)$ and $x_0 = \frac{D}{D+a_0}(s_0^{\text{in}} - s_0), x_1 = \frac{D}{D+a_1}(s_0^{\text{in}} - s_0 + s_1^{\text{in}} - s_1), x_2 = \frac{D}{D+a_2}((1 - \omega)(s_0^{\text{in}} - s_0) + s_1^{\text{in}} - s_1 + s_2^{\text{in}} - s_2)$
SS7	$s_0 = s_0^{\text{in}}$ and $s_2 = s_2^{\text{in}} + s_1^{\text{in}} - s_1$, where s_1 is a solution of $\psi_1(s_1) = D + a_1$ and $x_0 = 0, x_1 = \frac{D}{D+a_1}(s_1^{\text{in}} - s_1), x_2 = 0$
SS8	$s_0 = s_0^{\text{in}}, s_1 = \varphi_1(D), s_2 = M_2(D + a_2)$ and $x_0 = 0, x_1 = \frac{D}{D+a_1}(s_1^{\text{in}} - s_1), x_2 = \frac{D}{D+a_2}(s_1^{\text{in}} - s_1 + s_2^{\text{in}} - s_2)$

3. Mathematical analysis. In this section, the necessary and sufficient conditions of existence and stability of all steady states are given in Table 3. Any reference to steady state stability should be considered as local exponential stability, that is to say, the real parts of the eigenvalues of the Jacobian matrix are negative. We need the following notations:

$$(3.1) \quad \begin{aligned} E &= \frac{\partial \mu_0}{\partial s_0}(s_0, s_2), & F &= \frac{\partial \mu_0}{\partial s_2}(s_0, s_2), & G &= \frac{\partial \mu_1}{\partial s_1}(s_1, s_2), & H &= -\frac{\partial \mu_1}{\partial s_2}(s_1, s_2), \\ I &= \mu_2'(s_2), & J &= \mu_0(s_0, s_2), & K &= \mu_1(s_1, s_2), & L &= \mu_2(s_2). \end{aligned}$$

We have used the opposite sign of the partial derivative $H = -\partial \mu_1 / \partial s_2$, such that all constants involved in the computation become positive. Using the Liénard-Chipart stability criterion, the asymptotic stability of SS6 requires definitions and notations that are given in Table 2. Now, we can state our main result.

TABLE 2

Liénard-Chipart coefficients for SS6. The functions E, F, G, H, I, J, K and L , defined by (3.1), are evaluated at the components of SS6 given in Table 1. Notice that they are depending on the operating parameter D .

$$\begin{aligned}
c_1 &= 3D + (E + Fw)x_0 + (G + H)x_1 + Ix_2 \\
c_2 &= 3D^2 + (2D + J)(E + \omega F)x_0 + (2D + K)(G + H)x_1 + EIx_0x_2 + GIx_1x_2 \\
&\quad + (2D + L)Ix_2 + (E(G + H) - (1 - \omega)FG)x_0x_1 \\
c_3 &= D^3 + D(D + 2J)(E + \omega F)x_0 + D(D + 2K)(G + H)x_1 + D(D + 2L)Ix_2 \\
&\quad + EI(D + J + L)x_0x_2 + GI(D + K + L)x_1x_2 + EGIx_0x_1x_2 + (E(G + H) \\
&\quad - (1 - \omega)FG)(D + J + K)x_0x_1 \\
c_4 &= D^2(E + \omega F)Jx_0 + D^2(G + H)Kx_1 + D^2ILx_2 + EI(DJ + DL + JL)x_0x_2 \\
&\quad + GI(DK + DL + KL)x_1x_2 + EGI(J + K + L)x_0x_1x_2 + (E(G + H) \\
&\quad - (1 - \omega)FG)(DJ + DK + JK)x_0x_1 \\
c_5 &= DEIJLx_0x_2 + DGIKLx_1x_2 + D(E(G + H) - (1 - \omega)FG)JKx_0x_1 \\
&\quad + EGI(JK + JL + KL)x_0x_1x_2 \\
c_6 &= EGIJKLx_0x_1x_2 \\
\hline
r_0 &= c_1c_2 - c_3, \quad r_1 = c_1c_4 - c_5, \quad r_2 = c_3r_0 - c_1r_1, \quad r_3 = c_5r_0 - c_1^2c_6 \\
r_4 &= r_1r_2 - r_0r_3, \quad r_5 = r_3r_4 - c_1c_6r_2^2
\end{aligned}$$

160 *Theorem 3.1.* Assume that Hypotheses (H1) to (H8) hold. The necessary and
161 sufficient conditions of existence and local stability of the steady states are given in
162 [Table 3](#).

163 *Remark 3.2.* Let's recall that in [16] all steady states, except SS4, are unique.

- 164 • If $\omega \geq 1$, when it exists, SS4 is unique. Its stability condition $\frac{\partial \Psi}{\partial s_2}(s_2, D) > 0$ is
165 always satisfied.
- 166 • If $\omega < 1$, assuming also that (H8) holds, and if $(1 - \omega)s_0^{\text{in}} + s_1^{\text{in}} + s_2^{\text{in}} > \phi_1(D)$, the
167 equation defining s_2 in [Table 1](#) has two solutions $s_2^{*1} < s_2^{*2}$, such that $\frac{\partial \Psi}{\partial s_2}(s_2^{*1}, D) <$
168 0 and $\frac{\partial \Psi}{\partial s_2}(s_2^{*2}, D) > 0$. We denote by SS4¹ the steady state of type SS4 correspond-
169 ing to s_2^{*1} while SS4² corresponds to s_2^{*2} . When it exists, SS4¹ is unstable. When
170 SS4² exists, its stability condition $\frac{\partial \Psi}{\partial s_2}(s_2, D) > 0$ is always satisfied.
- 171 • The comparison with Table 4 of [16] shows that, with the exception of SS6, the
172 stability conditions of the steady states are the same as in the maintenance-free
173 case. Indeed, by replacing in the stability conditions of SS j , $j = 1, \dots, 8$, $j \neq 6$,
174 in [Table 3](#) the maintenance terms a_i by zero, for $i = 0, 1, 2$, we find the conditions
175 given in Table 4 of [16]. Therefore, the maintenance does not destabilize these
176 steady states. Only their regions of existence and stability, with respect to the
177 operating parameters, can be slightly modified when maintenance is included in
178 the model.

179 From [Table 3](#), we can deduce the following result.

180 *Proposition 3.3.*

- 181 • If SS2 or SS3 or SS7 exists then, SS1 is unstable.
- 182 • If SS6 exists then, SS2, SS4, SS5 and SS8 are unstable, when they exist.
- 183 • If SS5 exists then, SS2, SS3 and SS8 are unstable, when they exist.
- 184 • If SS8 exists then, SS7 is unstable, when it exists.

185 **4. Applications to a three-tiered microbial 'food web'.** In this section, we
186 consider the model of a chlorophenol-mineralising three-tiered microbial 'food web'
187 in a chemostat as application of our mathematical analysis, in order to compare our
188 findings to the numerical results in [26]. Let S_{ch} , S_{ph} and S_{H_2} be the chlorophenol,

TABLE 3

Existence and stability conditions of steady states of (1.1). The functions c_3 , c_5 , r_4 and r_5 are defined in Table 2. All other functions are given in Table 8.

	Existence conditions	Stability conditions
SS1	Always exists	$\mu_0(s_0^{\text{in}}, s_2^{\text{in}}) < D + a_0$, $\mu_1(s_1^{\text{in}}, s_2^{\text{in}}) < D + a_1$, $\mu_2(s_2^{\text{in}}) < D + a_2$
SS2	$\mu_2(s_2^{\text{in}}) > D + a_2$	$s_0^{\text{in}} < \varphi_0(D)$, $s_1^{\text{in}} < \varphi_1(D)$
SS3	$\mu_0(s_0^{\text{in}}, s_2^{\text{in}}) > D + a_0$	$\mu_1(s_0^{\text{in}} + s_1^{\text{in}} - s_0, s_2^{\text{in}} - \omega(s_0^{\text{in}} - s_0)) < D + a_1$, $s_2^{\text{in}} - \omega s_0^{\text{in}} < M_2(D + a_2) - \omega\varphi_0(D)$ with s_0 solution of $\psi_0(s_0) = D + a_0$
SS4	$(1 - \omega)s_0^{\text{in}} + s_1^{\text{in}} + s_2^{\text{in}} \geq \phi_1(D)$, $s_0^{\text{in}} > M_0(D + a_0, s_2)$, $s_0^{\text{in}} + s_1^{\text{in}} > M_0(D + a_0, s_2)$ $+ M_1(D + a_1, s_2)$ with s_2 solution of equation $\Psi(s_2, D) = (1 - \omega)s_0^{\text{in}} + s_1^{\text{in}} + s_2^{\text{in}}$	$(1 - \omega)s_0^{\text{in}} + s_1^{\text{in}} + s_2^{\text{in}} < \phi_2(D)$, $\phi_3(D) > 0$, $\frac{\partial \Psi}{\partial s_2}(s_2, D) > 0$
SS5	$s_0^{\text{in}} > \varphi_0(D)$, $s_2^{\text{in}} - \omega s_0^{\text{in}} > M_2(D + a_2) - \omega\varphi_0(D)$	$s_0^{\text{in}} + s_1^{\text{in}} < \varphi_0(D) + \varphi_1(D)$
SS6	$(1 - \omega)s_0^{\text{in}} + s_1^{\text{in}} + s_2^{\text{in}} > \phi_2(D)$, $s_0^{\text{in}} > \varphi_0(D)$, $s_0^{\text{in}} + s_1^{\text{in}} > \varphi_0(D) + \varphi_1(D)$	$c_3 > 0$, $c_5 > 0$, $r_4 > 0$, $r_5 > 0$
SS7	$\mu_1(s_1^{\text{in}}, s_2^{\text{in}}) > D + a_1$	$s_1^{\text{in}} + s_2^{\text{in}} < M_3(s_0^{\text{in}}, D + a_0)$ $+ M_1(D + a_1, M_3(s_0^{\text{in}}, D + a_0))$, $s_1^{\text{in}} + s_2^{\text{in}} < M_2(D + a_2) + \varphi_1(D)$
SS8	$s_1^{\text{in}} > \varphi_1(D)$, $s_1^{\text{in}} + s_2^{\text{in}} > \varphi_1(D) + M_2(D + a_2)$	$s_0^{\text{in}} < \varphi_0(D)$

189 phenol and hydrogen substrates concentrations. The specific growth rates take the
190 form:

$$191 \quad (4.1) \quad f_0(S_{\text{ch}}, S_{\text{H}_2}) = \frac{k_{m,\text{ch}} S_{\text{ch}}}{K_{S,\text{ch}} + S_{\text{ch}}} \frac{S_{\text{H}_2}}{K_{S,\text{H}_2,c} + S_{\text{H}_2}},$$

$$192 \quad f_1(S_{\text{ph}}, S_{\text{H}_2}) = \frac{k_{m,\text{ph}} S_{\text{ph}}}{K_{S,\text{ph}} + S_{\text{ph}}} \frac{1}{1 + S_{\text{H}_2}/K_{I,\text{H}_2}}, \quad f_2(S_{\text{H}_2}) = \frac{k_{m,\text{H}_2} S_{\text{H}_2}}{K_{S,\text{H}_2} + S_{\text{H}_2}}.$$

193 Let X_{ch} , X_{ph} and X_{H_2} be the chlorophenol, phenol and hydrogen degrader concen-
194 trations; $S_{\text{ch}}^{\text{in}}$, $S_{\text{ph}}^{\text{in}}$ and $S_{\text{H}_2}^{\text{in}}$ be the input concentrations; $k_{\text{dec, ch}}$, $k_{\text{dec, ph}}$ and $k_{\text{dec, H}_2}$ be
195 the decay rates. This model in [26] is described by the following system of differential
196 equations

$$197 \quad (4.2) \quad \begin{cases} \dot{X}_{\text{ch}} = (Y_{\text{ch}} f_0(S_{\text{ch}}, S_{\text{H}_2}) - D - k_{\text{dec, ch}}) X_{\text{ch}} \\ \dot{X}_{\text{ph}} = (Y_{\text{ph}} f_1(S_{\text{ph}}, S_{\text{H}_2}) - D - k_{\text{dec, ph}}) X_{\text{ph}} \\ \dot{X}_{\text{H}_2} = (Y_{\text{H}_2} f_2(S_{\text{H}_2}) - D - k_{\text{dec, H}_2}) X_{\text{H}_2} \\ \dot{S}_{\text{ch}} = D(S_{\text{ch}}^{\text{in}} - S_{\text{ch}}) - f_0(S_{\text{ch}}, S_{\text{H}_2}) X_{\text{ch}} \\ \dot{S}_{\text{ph}} = D(S_{\text{ph}}^{\text{in}} - S_{\text{ph}}) + \frac{224}{208}(1 - Y_{\text{ch}}) f_0(S_{\text{ch}}, S_{\text{H}_2}) X_{\text{ch}} - f_1(S_{\text{ph}}, S_{\text{H}_2}) X_{\text{ph}} \\ \dot{S}_{\text{H}_2} = D(S_{\text{H}_2}^{\text{in}} - S_{\text{H}_2}) - \frac{16}{208} f_0(S_{\text{ch}}, S_{\text{H}_2}) X_{\text{ch}} + \frac{32}{224}(1 - Y_{\text{ph}}) f_1(S_{\text{ph}}, S_{\text{H}_2}) X_{\text{ph}} \\ \quad - f_2(S_{\text{H}_2}) X_{\text{H}_2}, \end{cases}$$

198 where Y_{ch} , Y_{ph} and Y_{H_2} are the yield coefficients, respectively; $224/208(1 - Y_{\text{ch}})$ rep-
199 represents the fraction of chlorophenol converted to phenol; $32/224(1 - Y_{\text{ph}})$ represents
200 the fraction of phenol that is transformed to hydrogen and $16/208$ represents the frac-
201 tion of hydrogen consumed by the chlorophenol degrader. The biological parameter
202

203 values, used in [26], are provided in Table 15. Following [20], the rescaling of the vari-
 204 ables (G.1) and (G.2) can reduce (4.2) to the form (1.1), that is, the yields coefficients
 205 in (4.2) are normalized to one, except one of them which is equal to $\omega \simeq 0.53$. Under
 206 this rescaling (G.1) and (G.2), the growth functions (4.1) take the form (G.3) keep-
 207 ing their form of a double Monod, a Monod with product inhibition, and a Monod
 208 kinetics, respectively, so that Hypotheses (H1) to (H8) are satisfied. Therefore, with
 209 $\omega < 1$, Theorem 3.1 apply and give rigorous proofs for the results of [26], on exist-
 210 tence and stability of steady states, which, for the most part, have only been obtained
 211 numerically. See Appendix G for the details.

212 In the following, we consider $S_{ph}^{in} = 0$ and $S_{H_2}^{in} = 2.67 \times 10^{-5}$, corresponding to
 213 Fig. 3(a) in [26] and we fix $S_{ch}^{in} = 0.1$. Then, we determine the bifurcation diagram,
 214 where the operating parameter D is the bifurcation parameter. Our aim is to compare
 215 our results to those of [26] and to see if there are interesting phenomena that were
 216 not detected in the operating diagram depicted in Fig. 3(a) of [26], see Remark 4.2.
 217 Using Theorem 3.1, we have the following result, which is supported by numerical
 218 experimentation and is proved in Appendix D.

219 *Proposition 4.1.* Let $S_{ph}^{in} = 0$, $S_{H_2}^{in} = 2.67 \times 10^{-5}$ and $S_{ch}^{in} = 0.1$. In this case,
 220 SS7 and SS8 do not exist. Using the biological parameter values in Table 15, the
 221 bifurcation values δ_i , $i = 1, \dots, 7$ are provided in Table 4. The bifurcation analysis of
 222 (4.2) according to D is given in Table 5. The bifurcation types at the critical values
 223 δ_i are defined in Table 6.

TABLE 4

Critical parameter values δ_i , for $i = 1, \dots, 7$ where Y is defined in Appendix G, r_5 in Table 2 while all other functions are given in Table 8.

Definition	Value
δ_1 is the largest root of equation $r_5 = 0$	0.010412
δ_2 is the root of $\phi_2(D) - S_{H_2}^{in} - (1 - \omega)Y S_{ch}^{in} = 0$	0.068641
δ_3 is the root of $\phi_1(D) - S_{H_2}^{in} - (1 - \omega)Y S_{ch}^{in} = 0$	0.068814
δ_4 is the root of $S_{H_2}^{in} + \omega(\varphi_0(D) - Y S_{ch}^{in}) - M_2(D + a_2) = 0$	0.267251
δ_5 is the root of $\varphi_0(D) - Y S_{ch}^{in} = 0$	0.267636
$\delta_6 = \mu_0(Y S_{ch}^{in}, S_{H_2}^{in}) - a_0$	0.327130
$\delta_7 = \mu_2(S_{H_2}^{in}) - a_2$	1.064526

TABLE 5

Existence and stability of steady states, with respect to D . The bifurcation values δ_i , $i = 1, \dots, 7$ are given in Table 4. The letter S (resp. U) means that the corresponding steady state is stable (resp. unstable). No letter means that the steady state does not exist.

Interval	SS1	SS2	SS3	SS4 ¹	SS4 ²	SS5	SS6
$0 < D < \delta_1$	U	U	S	U	U		U
$\delta_1 < D < \delta_2$	U	U	S	U	U		S
$\delta_2 < D < \delta_3$	U	U	S	U	S		
$\delta_3 < D < \delta_4$	U	U	S				
$\delta_4 < D < \delta_5$	U	U	U			S	
$\delta_5 < D < \delta_6$	U	S	U				
$\delta_6 < D < \delta_7$	U	S					
$\delta_7 < D$	S						

TABLE 6

Bifurcation types corresponding to the critical values of δ_i , $i = 1, \dots, 7$, defined in Table 4. There exists also a critical value $\delta^* \simeq 0.009879 < \delta_1$ corresponding to the value of D where the stable limit cycle disappears when D is increasing.

Bifurcation types	
δ^*	Disappearance of the stable limit cycle
δ_1	Supercritical Hopf bifurcation
δ_2	Transcritical bifurcation of $SS4^2$ and $SS6$
δ_3	Saddle-node bifurcation of $SS4^1$ and $SS4^2$
δ_4	Transcritical bifurcation of $SS3$ and $SS5$
δ_5	Transcritical bifurcation of $SS2$ and $SS5$
δ_6	Transcritical bifurcation of $SS1$ and $SS3$
δ_7	Transcritical bifurcation of $SS1$ and $SS2$

224 Figure 4.1 shows the one-parameter bifurcation diagram of X_{ch} versus D in system
 225 (4.2). The magnifications of the bifurcation diagram are illustrated in Figure 4.1(b-
 226 c-d) showing the disappearance of the limit cycle at δ^* , the Hopf bifurcation at δ_1 ,
 227 the transcritical bifurcations at δ_2 , δ_4 and δ_5 and the saddle-node bifurcation at δ_3 .
 228 In Figure 4.1, $SS1$ and $SS2$ cannot be distinguished since they have both a zero X_{ch} -
 229 component. As $SS2$ is stable and $SS1$ is unstable for $D < \delta_7$, the $X_{ch} = 0$ axis is
 230 plotted in blue as the color of $SS2$ in Table 7.

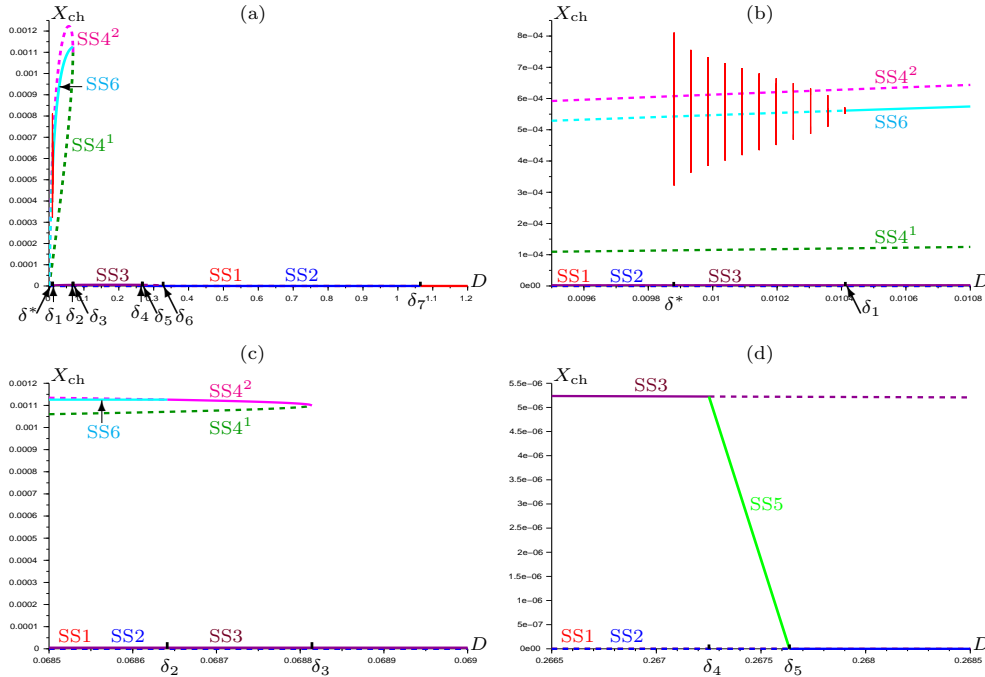


FIG. 4.1. (a) Bifurcation diagram of X_{ch} versus $D \in [0, 1.2]$ in model (4.2). (b) Magnification on the appearance and disappearance of stable limit cycles for $D \in [0.0095, 0.0108]$. (c) Magnification on the transcritical bifurcation at $D = \delta_2$ and the saddle-node bifurcation at $D = \delta_3$ for $D \in [0.0685, 0.069]$. (d) Magnification on the transcritical bifurcations for $D \in [0.2665, 0.2685]$.

TABLE 7

Colors used in [Figures 4.1 and E.1](#). The solid (resp. dashed) lines are used for stable (resp. unstable) steady states.

SS1	SS2	SS3	SS4 ¹	SS4 ²	SS5	SS6
Red	Blue	Purple	Dark Green	Magenta	Green	Cyan

For $S_{\text{ch}}^{\text{in}} = 0.1$, the operating diagram of Fig. 3(a) in [26] predicts only three possible behaviors: the stability of SS2, the stability of SS3 and the bistability between SS3 and SS6. Note that the destabilization of SS6 via a Hopf bifurcation with emergence of a stable limit cycle has not been observed in [26]. Moreover, the region of existence and stability of SS5, which was depicted in Fig. 3(b) of [26] in the case where $S_{\text{H}_2}^{\text{in}} = 2.67 \times 10^{-2}$, was not reported in Fig. 3(a) of [26]. Our results show that this region also exists when $S_{\text{H}_2}^{\text{in}} = 2.67 \times 10^{-5}$, and explain why it was not detected by the numerical analysis given in Fig. 3(a) of [26]: SS5 occurs in a very small region since, for $S_{\text{ch}}^{\text{in}} = 0.1$ it corresponds to $\delta_4 < D < \delta_5$, where $\delta_4 \simeq 0.267251$ and $\delta_5 \simeq 0.267636$, with $\delta_5 - \delta_4$ of order 10^{-4} . However, while from a mathematical point of view the diagram shown in [26] is incorrectly labeled, in biological terms, such a small region of SS5 would likely not be attained.

To compare our results to those achieved in [16], we determine the bifurcation diagram in [Appendix E](#) according to the bifurcation parameter $S_{\text{ch}}^{\text{in}}$. Further, numerical simulations are presented in [Figures 4.2 to 4.4](#) (see also [Figures H.1 to H.4](#)) to illustrate our findings, where the bifurcation values σ_5 , σ_6 and σ^* of $S_{\text{ch}}^{\text{in}}$ are provided in [Tables 10 and 12](#), respectively. We illustrate, in particular, the interesting three cases where the steady states SS1, SS2, SS4¹ and SS4² are unstable:

- For $S_{\text{ch}}^{\text{in}} \in (\sigma_5, \sigma^*)$, the numerical simulations done for various positive initial conditions permit to conjecture the global asymptotic stability of SS3 (see [Figure 4.2](#)).
- For $S_{\text{ch}}^{\text{in}} \in (\sigma^*, \sigma_6)$, the system exhibits a bistability with two basins of attraction: one toward the stable limit cycle and the second toward SS3. [Figure 4.3](#) illustrates that the trajectories in pink and blue converge toward the stable limit cycle in red, while the green trajectory converges toward SS3. For the initial condition in [Table 14](#), the time course in [Figure H.1](#) illustrates the positive, periodic solution representing the coexistence of the three species. The sustained oscillations prove the stability of the limit cycle. However, [Figure H.2](#) shows the time course of the green trajectory in [Figure 4.3](#).
- For $S_{\text{ch}}^{\text{in}} > \sigma_6$, the system exhibits a bistability between SS6 and SS3. [Figure 4.4](#) shows that the blue trajectory converges to the stable focus SS6, while the green trajectory converges to SS3. [Figures H.3 and H.4](#) illustrate the time courses corresponding to the blue and the green trajectories in [Figure 4.4](#), respectively.

Numerical simulations have shown that the stable limit cycle disappears at the critical value $\sigma^* \in (\sigma_5, \sigma_6)$ as $S_{\text{ch}}^{\text{in}}$ decreases. Similarly to the numerical study of the bifurcation diagram with respect to the parameter D in [23] in the case without maintenance and $s_1^{\text{in}} = s_2^{\text{in}} = 0$, we conjecture that in our case also the stable limit cycle disappears through a saddle-node bifurcation with another unstable limit cycle when $S_{\text{ch}}^{\text{in}}$ decreases.

5. Conclusion. In this study, we discussed the dynamics of three interacting microbial species describing a chlorophenol-mineralising three-tiered ‘food web’ in the chemostat (4.2), introduced by Wade et al. [26] following previous work on a

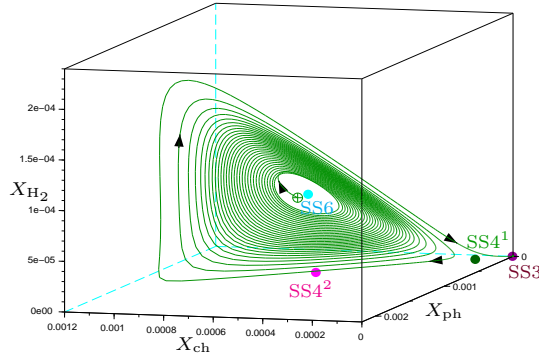


FIG. 4.2. Case $S_{ch}^{in} = 0.098 < \sigma^*$: the solution of (4.2) converges to $SS3$.

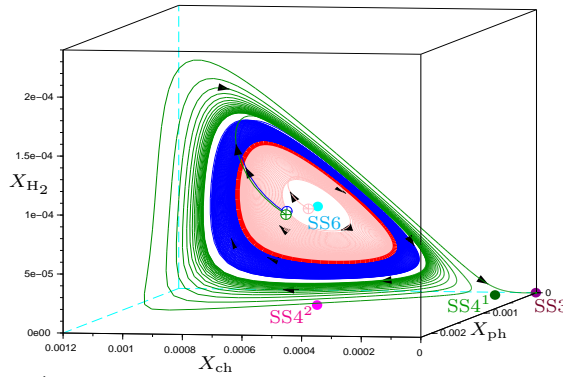


FIG. 4.3. Case $\sigma^* < S_{ch}^{in} = 0.0995 < \sigma_6$: bistability with convergence either to the stable limit cycle (in red) or to $SS3$.

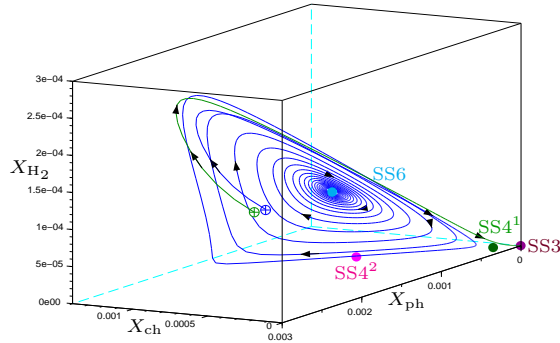


FIG. 4.4. Case $\sigma_6 < S_{ch}^{in} = 0.11$: bistability with convergence either to $SS6$ or to $SS3$.

274 two-tiered model [29]. The existence and stability of the steady states of model
 275 (4.2) have been analyzed as a function of the operating parameters (input substrate
 276 concentrations and dilution rate), using numerical tools and specific values of the
 277 biological parameters.

278 In this paper, we gave a complete analysis of the dynamics of the model (1.1)
 279 which generalizes (4.2) by allowing a larger class of growth functions. The existence
 280 of the steady states was analytically characterized in [16] where it was shown that
 281 model (1.1) can have up to eight types of steady states: the washout steady state

282 denoted by SS1, six types of boundary steady states where one or two degrader popu-
283 lations are extinct denoted by SS2, SS3, SS4, SS5, SS7 and SS8, and a positive steady
284 state, denoted by SS6, where all microbial populations coexist. When they exist, all
285 steady states are unique, except the steady state SS4 where chlorophenol and phenol
286 degraders are maintained and the hydrogen degrader is eliminated.

287 Here, we focus on the stability of steady states. We have managed to characterize
288 the stability in this six-dimensional system, although it is generally accepted that
289 the Routh–Hurwitz theorem is intractable beyond five dimensions. For this, we have
290 used the Liénard–Chipart stability criterion to simplify the mathematical analysis by
291 reducing considerably the number of the Routh–Hurwitz conditions to check. For SS1,
292 SS2, SS3 and SS7, the stability conditions are determined explicitly. For SS4, SS5
293 and SS8, we explicitly characterize the stability conditions using the Liénard–Chipart
294 stability criterion. For SS6, the stability is given with respect to the signs of the
295 Liénard–Chipart coefficients by using numerical experimentation (see [Appendix D](#)) to
296 plot these coefficients, whose signs cannot be determined analytically. As shown in
297 [Appendix G](#), our presentation of the existence and stability issue fully clarifies the
298 numerical study made in [26] on the three-tiered ‘food web’ model (4.2).

299 Our work extends all results on the stability of the existing literature [8, 16, 20, 23],
300 which were obtained only in the case without maintenance, where the six-dimensional
301 system (1.1) can be reduced to a three-dimensional one. We show that for SS4,
302 which can exist in two forms, at most one steady state can be stable, a fact that was
303 already noticed (when maintenance is not included in the model) in the particular
304 case without phenol and hydrogen input concentrations, studied in [20] and in the
305 general case, where these input concentrations are added, studied in [16].

306 We highlighted several possible asymptotic behaviors in this six-dimensional sys-
307 tem, including the bistability between the positive steady state and a boundary steady
308 state, or the bistability between a positive limit cycle and a boundary steady state,
309 so that the long term behavior depends on the initial condition. We proved that the
310 positive steady state of coexistence of all species can be unstable and we give numeri-
311 cal evidence for the supercritical Hopf bifurcation, in the case including chlorophenol
312 and hydrogen input concentrations. The possibility of the Hopf bifurcation of the
313 positive steady state was previously observed in [20] in the case without phenol and
314 hydrogen input concentrations.

315 In order to gain more insight into the behavior of the system, we give a bifurcation
316 diagram with the dilution rate as the bifurcating parameter (see [Figure 4.1](#)) showing
317 that one of the operating diagrams obtained numerically in [26] has omitted important
318 transition phenomena between steady states. If the dilution rate is too low, only the
319 chlorophenol degrader is maintained (SS3 is the only stable steady state). Increasing
320 slightly the dilution rate D , the system exhibits a bistability behavior where either
321 only the chlorophenol degrader is maintained (SS3 is stable) or the coexistence of
322 three microbial species may occur around periodic oscillations (SS6 is unstable and a
323 stable limit cycle exists). Increasing a little more D , the system exhibits a bistability
324 behavior where either only the chlorophenol degrader is maintained or the coexistence
325 of three microbial species occurs at the positive steady state (SS3 and SS6 are both
326 stable). Increasing further D , the system exhibits a bistability between only the
327 chlorophenol degrader and both the chlorophenol and phenol degraders (SS3 and SS4²
328 are both stable). Rising a little more the value of D , only the chlorophenol degrader
329 is maintained. Then, only the chlorophenol and hydrogen degraders are maintained
330 (SS5 is the only stable steady state). Adding a little more, both the chlorophenol and
331 phenol degraders are eliminated from the reactor and only the hydrogen degrader is

332 maintained, since $S_{H_2}^{\text{in}} > 0$ (SS2 is the only stable steady state). For higher dilution
 333 rate, there is washout of all three microbial populations (SS1 is the only stable steady
 334 state).

335 Our results show that with the exception of SS6, the maintenance does not desta-
 336 bilize the steady states. To make our theoretical results useful in practice, it would
 337 be necessary to have the description of the operating diagrams that give the regions
 338 of existence and stability of the steady states, in the space of the operating parame-
 339 ters. In a future work, we will use our results to determine analytically the operating
 340 diagrams in the cases with and without maintenance. These operating diagrams will
 341 also allow us to answer the delicate question of whether or not SS6 can be destabilized
 342 by including maintenance terms. Even without maintenance, this steady state can
 343 be stable or unstable depending on the values of the operating parameters. Does the
 344 introduction of maintenance modify the boundary between the region of stability and
 345 the region of instability, or does it make more complex phenomena appear?

346 **Appendix A. Auxiliary functions.** For the description of the steady states
 347 given in Table 1, together with the statement of their conditions of existence and
 348 stability, we need to define some auxiliary functions that are listed in Table 8. Using
 349 Hypotheses (H1) to (H7), the existence and definition domains of these functions are
 all relatively straightforward and can be found as in [20].

TABLE 8
 Notations, intervals and auxiliary functions.

Definition	
$s_i = M_i(y, s_2)$ $i = 0, 1$	Let $s_2 \geq 0$. $s_i = M_i(y, s_2)$ is the unique solution of $\mu_i(s_i, s_2) = y$, for all $0 \leq y < \mu_i(+\infty, s_2)$
$s_2 = M_2(y)$	$s_2 = M_2(y)$ is the unique solution of $\mu_2(s_2) = y$, for all $0 \leq y < \mu_2(+\infty)$
$s_2 = M_3(s_0, z)$	Let $s_0 \geq 0$. $s_2 = M_3(s_0, z)$ is the unique solution of $\mu_0(s_0, s_2) = z$, for all $0 \leq z < \mu_0(s_0, +\infty)$
$s_2^i = s_2^i(D)$ $i = 0, 1$	$s_2^i = s_2^i(D)$ is the unique solution of $\mu_i(+\infty, s_2) = D + a_i$, for all $D + a_0 < \mu_0(+\infty, +\infty)$, $\mu_1(+\infty, +\infty) < D + a_1 < \mu_1(+\infty, 0)$, resp.
I_1, I_2	$I_1 = \{D \geq 0 : s_2^0 < s_2^1\}$, $I_2 = \{D \in I_1 : s_2^0 < M_2(D + a_2) < s_2^1\}$
$\Psi(s_2, D)$	$\Psi(s_2, D) = (1 - \omega)M_0(D + a_0, s_2) + M_1(D + a_1, s_2) + s_2$, for all $D \in I_1$ and $s_2^0 < s_2 < s_2^1$
$\phi_1(D)$	$\phi_1(D) = \inf_{s_2^0 < s_2 < s_2^1} \Psi(s_2, D)$, for all $D \in I_1$
$\phi_2(D)$	$\phi_2(D) = \Psi(M_2(D + a_2), D)$, for all $D \in I_2$
$\phi_3(D)$	$\phi_3(D) = \frac{\partial \Psi}{\partial s_2}(M_2(D + a_2), D)$, for all $D \in I_2$
J_0, J_1	$J_0 = (\max(0, s_0^{\text{in}} - s_2^{\text{in}}/\omega), s_0^{\text{in}})$, $J_1 = (0, s_1^{\text{in}})$
$\psi_0(s_0)$	$\psi_0(s_0) = \mu_0(s_0, s_2^{\text{in}} - \omega(s_0^{\text{in}} - s_0))$, for all $s_0 \geq \max(0, s_0^{\text{in}} - s_2^{\text{in}}/\omega)$
$\psi_1(s_1)$	$\psi_1(s_1) = \mu_1(s_1, s_2^{\text{in}} + s_1^{\text{in}} - s_1)$, for all $s_1 \in [0, s_1^{\text{in}} + s_2^{\text{in}}]$
$\varphi_i(D)$ $i = 0, 1$	$\varphi_i(D) = M_i(D + a_i, M_2(D + a_2))$, resp., for all, $D \in \{D \geq 0 : s_2^0 < M_2(D + a_2)\}$, $D \in \{D \geq 0 : M_2(D + a_2) < s_2^1\}$

350

351 **Appendix B. Liénard-Chipart stability criterion.** Note that conditions
 352 in the stability criterion of Liénard and Chipart (see Gantmacher [10], Theorem 11)
 353 represent almost half that of the Routh–Hurwitz theorem which facilitates the study
 354 of asymptotic behavior of dynamic systems especially for dimensions beyond five. It
 355 is known that for a polynomial of degree four the Routh–Hurwitz conditions can be
 356 written as in the following Lemma, see, for instance, Theorem 11 [6].

Lemma B.1. Consider the fourth-order polynomial $P(\lambda)$ with real coefficients given by:

$$P(\lambda) = c_0\lambda^4 + c_1\lambda^3 + c_2\lambda^2 + c_3\lambda + c_4.$$

All of the roots of the polynomial $P(\lambda)$ have negative real part if and only if

$$(B.1) \quad c_i > 0, \quad \text{for } i = 1, 3, 4, \quad \text{and} \quad r_1 = c_3(c_1c_2 - c_0c_3) - c_1^2c_4 > 0.$$

The following Lemma gives the conditions of stability for a six-dimensional dynamic system.

Lemma B.2. Consider the six-order polynomial $P(\lambda)$ with real coefficients given by:

$$P(\lambda) = c_0\lambda^6 + c_1\lambda^5 + c_2\lambda^4 + c_3\lambda^3 + c_4\lambda^2 + c_5\lambda + c_6.$$

All of the roots of the polynomial $P(\lambda)$ have negative real part if and only if

$$(B.2) \quad c_i > 0, \quad i = 1, 3, 5, 6, \quad r_4 > 0 \quad \text{and} \quad r_5 > 0,$$

where $r_4 = r_1r_2 - r_0r_3$ and $r_5 = r_3r_4 - c_1c_6r_2^2$, with

$$r_0 = c_1c_2 - c_0c_3, \quad r_1 = c_1c_4 - c_0c_5, \quad r_2 = c_3r_0 - c_1r_1 \quad \text{and} \quad r_3 = c_5r_0 - c_1^2c_6.$$

Proof. From the Liénard-Chipart stability criterion, all of the roots of the polynomial P have negative real part if and only if

$$(B.3) \quad c_i > 0, \quad i = 1, 3, 5, 6, \quad \det(\Delta_2) > 0, \quad \det(\Delta_4) > 0 \quad \text{and} \quad \det(\Delta_6) > 0,$$

where Δ_2 , Δ_4 and Δ_6 are the Hurwitz matrices defined by:

$$\Delta_2 = \begin{bmatrix} c_1 & c_3 \\ c_0 & c_2 \end{bmatrix}, \quad \Delta_4 = \begin{bmatrix} c_1 & c_3 & c_5 & 0 \\ c_0 & c_2 & c_4 & c_6 \\ 0 & c_1 & c_3 & c_5 \\ 0 & c_0 & c_2 & c_4 \end{bmatrix}, \quad \Delta_6 = \begin{bmatrix} c_1 & c_3 & c_5 & 0 & 0 & 0 \\ c_0 & c_2 & c_4 & c_6 & 0 & 0 \\ 0 & c_1 & c_3 & c_5 & 0 & 0 \\ 0 & c_0 & c_2 & c_4 & c_6 & 0 \\ 0 & 0 & c_1 & c_3 & c_5 & 0 \\ 0 & 0 & c_0 & c_2 & c_4 & c_6 \end{bmatrix}.$$

Conditions (B.3) are equivalent to

$$(B.4) \quad c_i > 0, \quad i = 1, 3, 5, 6, \quad r_0 > 0, \quad r_4 = r_1r_2 - r_0r_3 > 0, \quad r_5 = r_3r_4 - c_1c_6r_2^2 > 0.$$

When all conditions (B.4) hold, the condition $r_5 > 0$ implies that $r_3 > 0$, that is, $c_5r_0 > c_6c_1^2$ which implies that $r_0 > 0$. Hence, conditions (B.4) are equivalent to (B.2). \square

Appendix C. Proofs.

C.1. Proof of Theorem 3.1. The existence of the steady states is proven in [16]. The local stability of the steady states is determined by the eigenvalues of the Jacobian matrix of system (1.1) evaluated at the steady state. The Jacobian matrix of (1.1) corresponds to the 6×6 matrix:

$$\mathcal{J} = \begin{bmatrix} J-D-a_0 & 0 & 0 & Ex_0 & 0 & Fx_0 \\ 0 & K-D-a_1 & 0 & 0 & Gx_1 & -Hx_1 \\ 0 & 0 & L-D-a_2 & 0 & 0 & Ix_2 \\ -J & 0 & 0 & -D-Ex_0 & 0 & -Fx_0 \\ J & -K & 0 & Ex_0 & -D-Gx_1 & Fx_0+Hx_1 \\ -\omega J & K & -L & -\omega Ex_0 & Gx_1 & -D-\omega Fx_0-Hx_1-Ix_2 \end{bmatrix},$$

383 where the functions E, F, G, H, I, J, K and L are defined by (3.1), and are evaluated
 384 at the steady state. The stability of the steady state is investigated by analyzing the
 385 real parts of the eigenvalues of \mathcal{J} , which are the roots of the characteristic polynomial.

For SS1, the characteristic polynomial is

$$P_1(\lambda) = (\lambda - \lambda_1)(\lambda - \lambda_2)(\lambda - \lambda_3)(\lambda + D)^3,$$

386 where $\lambda_1 = \mu_0(s_0^{\text{in}}, s_2^{\text{in}}) - D - a_0$, $\lambda_2 = \mu_1(s_1^{\text{in}}, s_2^{\text{in}}) - D - a_1$ and $\lambda_3 = \mu_2(s_2^{\text{in}}) - D - a_2$.
 387 Therefore, SS1 is stable if and only if $\lambda_1 < 0$, $\lambda_2 < 0$ and $\lambda_3 < 0$, that is, the stability
 388 conditions of SS1 in Table 3 hold.

For SS2, the characteristic polynomial is

$$P_2(\lambda) = (\lambda - \lambda_1)(\lambda - \lambda_2)(\lambda + D)^2(\lambda^2 + c_1\lambda + c_2),$$

389 where $c_1 = D + Ix_2$, $c_2 = LIx_2$ and

$$390 \text{ (C.1) } \lambda_1 = \mu_0(s_0^{\text{in}}, M_2(D + a_2)) - D - a_0, \quad \lambda_2 = \mu_1(s_1^{\text{in}}, M_2(D + a_2)) - D - a_1,$$

392 Since $c_1 > 0$ and $c_2 > 0$, the real parts of the roots of the quadratic factor are
 393 negative. Therefore, SS2 is stable if and only if $\lambda_1 < 0$ and $\lambda_2 < 0$. Since M_0 and
 394 M_1 are increasing, these conditions are equivalent to the stability conditions of SS2
 395 in Table 3.

For SS3, the characteristic polynomial is

$$P_3(\lambda) = (\lambda - \lambda_1)(\lambda - \lambda_2)(\lambda + D)^2(\lambda^2 + c_1\lambda + c_2),$$

396 where

397 $\lambda_1 = \mu_1(s_0^{\text{in}} - s_0 + s_1^{\text{in}}, s_2^{\text{in}} - \omega(s_0^{\text{in}} - s_0)) - D - a_1$, $\lambda_2 = \mu_2(s_2^{\text{in}} - \omega(s_0^{\text{in}} - s_0)) - D - a_2$,
 398 $c_1 = D + (E + \omega F)x_0$ and $c_2 = J(E + \omega F)x_0$, where s_0 is the solution in the interval
 399 J_0 of equation $\psi_0(s_0) = D + a_0$. Since $c_1 > 0$ and $c_2 > 0$, the real parts of the roots
 400 of the quadratic factor are negative. Therefore, SS3 is stable if and only if $\lambda_1 < 0$ and
 401 $\lambda_2 < 0$. The condition $\lambda_1 < 0$ is the first stability condition of SS3 in Table 3. Since
 402 M_2 is increasing, the condition $\lambda_2 < 0$ is equivalent to

$$403 \text{ (C.2) } s_2^{\text{in}} - \omega(s_0^{\text{in}} - s_0) < M_2(D + a_2) \iff s_0 < (M_2(D + a_2) - s_2^{\text{in}}) / \omega + s_0^{\text{in}}.$$

405 As the function ψ_0 is increasing, (C.2) is equivalent to

$$406 \text{ (C.3) } \psi_0(s_0) < \psi_0((M_2(D + a_2) - s_2^{\text{in}}) / \omega + s_0^{\text{in}}).$$

From the definition of the function ψ_0 together with the condition $\psi_0(s_0) = D + a_0$
 defining s_0 , we deduce that (C.3) is equivalent to

$$D + a_0 < \mu_0((M_2(D + a_2) - s_2^{\text{in}}) / \omega + s_0^{\text{in}}, M_2(D + a_2)).$$

408 Since M_0 is increasing, this condition is equivalent to the second stability condition
 409 of SS3 in Table 3.

For SS4, the characteristic polynomial is

$$P_4(\lambda) = (\lambda - \lambda_1)(\lambda + D)(\lambda^4 + c_1\lambda^3 + c_2\lambda^2 + c_3\lambda + c_4),$$

410 where $\lambda_1 = \mu_2(s_2) - D - a_2$ with s_2 is defined in Table 1 and the coefficients c_i for
 411 $i = 1, \dots, 4$ are given by

$$412 c_1 = 2D + (E + \omega F)x_0 + (G + H)x_1,$$

$$413 c_2 = D^2 + (E + \omega F)(D + J)x_0 + (G + H)(D + K)x_1 + (E(G + H) - (1 - \omega)FG)x_0x_1,$$

$$414 c_3 = D(E + \omega F)Jx_0 + D(G + H)Kx_1 + (E(G + H) - (1 - \omega)FG)(J + K)x_0x_1,$$

$$415 c_4 = (E(G + H) - (1 - \omega)FG)JKx_0x_1.$$

417 From Lemma B.1, all of the roots of the fourth order polynomial have negative real
418 parts if and only if

$$419 \quad (C.4) \quad c_i > 0, \quad \text{for } i = 1, 3, 4 \quad \text{and} \quad r_1 = c_1 c_2 c_3 - c_1^2 c_4 - c_3^2 > 0.$$

421 We always have $c_1 > 0$. Moreover, $c_3 > 0$ and $c_4 > 0$ if and only if

$$422 \quad (C.5) \quad E(G + H) - (1 - \omega)FG > 0.$$

424 Let us denote

$$425 \quad A = G + H, \quad B = \frac{E(G+H)-(1-\omega)FG}{G+H} \quad \text{and} \quad C = \frac{G+\omega H}{G+H} F.$$

426 Note that $B > 0$ if and only if condition (C.5) is satisfied. Then, we can write c_i , for
427 $i = 1, \dots, 4$ as follows:

$$\begin{aligned} 428 \quad c_1 &= 2D + (B + C)x_0 + Ax_1, \\ 429 \quad c_2 &= D^2 + (B + C)(D + J)x_0 + A(D + K)x_1 + ABx_0x_1, \\ 430 \quad c_3 &= D(B + C)Jx_0 + DAKx_1 + AB(J + K)x_0x_1, \quad c_4 = ABJKx_0x_1. \end{aligned}$$

432 We can write r_1 as follows:

$$\begin{aligned} 433 \quad r_1 &= DJ[(D + J)(B + C)^3 - B^3J]x_0^3 + D^2A^3Kx_1^3 + B^2A^2(B + C)(J + K)x_0^3x_1^2 + B^2A^3(J + K)x_0^2x_1^3 \\ &+ BA[D(2J + K)(B + C)^2 + CJ^2(2B + C)]x_0^3x_1 + DBA^3(J + 2K)x_0x_1^3 + 3D^3A^2Kx_1^2 \\ &+ D^2J[3D(B + C)^2 + CJ(2B + C)]x_0^2 + BA^2[D(J + K)(5B + 3C) + C(J^2 + K^2)]x_0^2x_1^2 \\ &+ DA[C(DC(2J + K) + CJ(J + 2K) + DB(9J + 5K) + 2BJ^2) + DB^2(7J + 4K)]x_0^2x_1 \\ &+ DA^2[DB(4J + 7K) + CK(2J + K) + DC(J + 2K)]x_0x_1^2 + 2D^4J(B + C)x_0 + 2D^4AKx_1 \\ &+ D^2A[D(J + K)(5B + 3C) + 2CJK]x_0x_1 + (D^2 + DBx_0 + DAx_1 + BAx_0x_1)(BJx_0 - AKx_1)^2. \end{aligned}$$

434 Hence, conditions (C.4) are verified if and only if (C.5) is satisfied. Let us prove that
435 condition (C.5) is equivalent to $\frac{\partial \Psi}{\partial s_2}(s_2, D) > 0$. Let $s_2 > 0$. Under (H4) and (H5),
436 we have

$$\begin{aligned} 437 \quad \frac{\partial M_0}{\partial s_2}(y, s_2) &= -\frac{\partial \mu_0}{\partial s_2}(M_0(y, s_2), s_2) \left[\frac{\partial \mu_0}{\partial s_0}(M_0(y, s_2), s_2) \right]^{-1}, \quad \text{for all } y \in (0, \mu_0(+\infty, s_2)), \\ \frac{\partial M_1}{\partial s_2}(y, s_2) &= -\frac{\partial \mu_1}{\partial s_2}(M_1(y, s_2), s_2) \left[\frac{\partial \mu_1}{\partial s_1}(M_1(y, s_2), s_2) \right]^{-1}, \quad \text{for all } y \in (0, \mu_1(+\infty, s_2)). \end{aligned}$$

Using (3.1), we obtain

$$\frac{\partial M_0}{\partial s_2}(D + a_0, s_2) = -\frac{F}{E} \quad \text{and} \quad \frac{\partial M_1}{\partial s_2}(D + a_1, s_2) = \frac{H}{G}.$$

438 Moreover, we have for all $s_2 \in (s_2^0, s_2^1)$ and $D \in I_1$,

$$439 \quad (C.6) \quad \frac{\partial \Psi}{\partial s_2}(s_2, D) = (1 - \omega) \frac{\partial M_0}{\partial s_2}(D + a_0, s_2) + \frac{\partial M_1}{\partial s_2}(D + a_1, s_2) + 1.$$

Using (C.6), it follows that

$$\frac{\partial \Psi}{\partial s_2}(s_2, D) = -\frac{F}{E}(1 - \omega) + \frac{H}{G} + 1 = \frac{E(G+H)-(1-\omega)FG}{EG}.$$

441 Since E and G are positive, condition (C.5) is equivalent to $\frac{\partial \Psi}{\partial s_2}(s_2, D) > 0$. Conse-
442 quently, since μ_2 is increasing, it follows that, SS4 is stable if and only if

$$443 \quad (C.7) \quad s_2 < M_2(D + a_2) \quad \text{and} \quad \frac{\partial \Psi}{\partial s_2}(s_2, D) > 0,$$

445 which is equivalent to the stability condition in [Table 3](#) because this first condition
 446 of [\(C.7\)](#) is equivalent the first and the second one of SS4 in [Table 3](#) (similarly to the
 447 proof of Theorem 2 in [\[16\]](#)).

For SS5, the characteristic polynomial is

$$P_5(\lambda) = (\lambda - \lambda_1)(\lambda + D) (\lambda^4 + c_1\lambda^3 + c_2\lambda^2 + c_3\lambda + c_4),$$

448 where $\lambda_1 = \mu_1 (s_0^{\text{in}} + s_1^{\text{in}} - M_0(D + a_0), M_2(D + a_2)) - D - a_1$ and the
 449 coefficients c_i are given by:

$$450 \quad c_1 = 2D + (E + \omega F)x_0 + Ix_2,$$

$$451 \quad c_2 = D^2 + (E + \omega F)(D + J)x_0 + I(D + L)x_2 + EIx_0x_2,$$

$$452 \quad c_3 = D(E + \omega F)Jx_0 + DILx_2 + EI(J + L)x_0x_2 \quad \text{and} \quad c_4 = EIJLx_0x_2.$$

454 From [Lemma B.1](#), the roots of the fourth order polynomial are of negative real parts
 455 if and only if

$$456 \quad (\text{C.8}) \quad c_i > 0, \quad \text{for} \quad i = 1, 3, 4 \quad \text{and} \quad r_1 = c_1c_2c_3 - c_1^2c_4 - c_3^2 > 0.$$

458 We always have $c_i > 0$ for $i = 1, 3, 4$. We can write r_1 as follows:

$$\begin{aligned} r_1 = & DJ [(D + J)(E + \omega F)^3 - E^3J] x_0^3 + D^2I^3Lx_2^3 + E^2I^2(E + \omega F)(J + L)x_0^3x_2^2 + DEI^3(J + 2L)x_0x_2^3 \\ & + E^2I^3(J + L)x_0^2x_2^3 + EI [D(2J + L)(E + \omega F)^2 + \omega FJ^2(2E + \omega F)] x_0^3x_2 + 3D^3I^2Lx_2^2 \\ & + D^2J [3D(E + \omega F)^2 + F\omega J(2E + \omega F)] x_0^2 + EI^2 [D(J + L)(5E + 3\omega F) + F\omega (J^2 + L^2)] x_0^2x_2^2 \\ 459 \quad & + DI [F\omega (DF\omega(2J + L) + F\omega J(J + 2L) + DE(9J + 5L) + 2EJ^2) + DE^2(7J + 4L)] x_0^2x_2 \\ & + DI^2 [DE(4J + 7L) + F\omega L(2J + L) + DF\omega(J + 2L)] x_0x_2^2 + 2D^4J(E + \omega F)x_0 + 2D^4ILx_2 \\ & + D^2I [D(J + L)(5E + 3\omega F) + 2F\omega JL] x_0x_2 + (D^2 + DEx_0 + DIx_2 + EIx_0x_2) (EJx_0 - ILx_2)^2. \end{aligned}$$

460 Thus, $r_1 > 0$. Consequently, the conditions [\(C.8\)](#) are satisfied. Therefore, SS5
 461 is stable if and only if $\lambda_1 < 0$. Since M_1 is increasing, this condition is equivalent to the
 462 stability condition of SS5 in [Table 3](#).

For SS6, the characteristic polynomial is given by:

$$P_6(\lambda) = \lambda^6 + c_1\lambda^5 + c_2\lambda^4 + c_3\lambda^3 + c_4\lambda^2 + c_5\lambda + c_6,$$

463 where c_i , $i = 1, \dots, 6$ are defined in [Table 2](#). From [Lemma B.2](#), all of the roots of the
 464 sixth order polynomial have negative real parts if and only if $c_i > 0$, $i = 1, 3, 5, 6$ and
 465 $r_j > 0$, $j = 4, 5$, where c_i and r_j are listed in [Table 2](#). Since c_1 and c_6 are positive,
 466 the proof is complete.

For SS7, the characteristic polynomial is

$$P_7(\lambda) = (\lambda - \lambda_1)(\lambda - \lambda_2)(\lambda + D)^2(\lambda^2 + c_1\lambda + c_2),$$

467 where $\lambda_1 = \mu_0 (s_0^{\text{in}}, s_1^{\text{in}} - s_1 + s_2^{\text{in}}) - D - a_0$, $\lambda_2 = \mu_2 (s_1^{\text{in}} - s_1 + s_2^{\text{in}}) - D - a_2$, $c_1 =$
 468 $D + (G + H)x_1$ and $c_2 = K(G + H)x_1$ where s_1 is the solution in the interval J_1 of
 469 equation $\psi_1(s_1) = D + a_1$. Since $c_1 > 0$ and $c_2 > 0$, the real parts of the roots of
 470 the quadratic factor are negative. Therefore, SS7 is stable if and only if $\lambda_1 < 0$ and
 471 $\lambda_2 < 0$. Since the functions M_2 and M_3 are increasing, the conditions $\lambda_1 < 0$ and
 472 $\lambda_2 < 0$ are equivalent to

$$473 \quad (\text{C.9}) \quad s_1 > s_1^{\text{in}} + s_2^{\text{in}} - M_3(s_0^{\text{in}}, D + a_0) \quad \text{and} \quad s_1 > s_1^{\text{in}} + s_2^{\text{in}} - M_2(D + a_2).$$

Since the function ψ_1 is increasing, (C.9) is equivalent to

$$\psi_1(s_1) > \psi_1(s_1^{\text{in}} + s_2^{\text{in}} - M_3(s_0^{\text{in}}, D + a_0)), \quad \psi_1(s_1) > \psi_1(s_1^{\text{in}} + s_2^{\text{in}} - M_2(D + a_2)).$$

475 From the definition of the function ψ_1 together with the condition $\psi_1(s_1) = D + a_1$
476 which defines s_1 , the preceding conditions are equivalent to

$$477 \quad \begin{aligned} \mu_1(s_1^{\text{in}} + s_2^{\text{in}} - M_3(s_0^{\text{in}}, D + a_0), M_3(s_0^{\text{in}}, D + a_0)) &< D + a_1, \\ \mu_1(s_1^{\text{in}} + s_2^{\text{in}} - M_2(D + a_2), M_2(D + a_2)) &< D + a_1. \end{aligned}$$

478 Since M_1 is increasing, these conditions are equivalent to the stability conditions of
479 SS7 in Table 3.

For SS8, the characteristic polynomial is

$$P_8(\lambda) = (\lambda - \lambda_1)(\lambda + D) (\lambda^4 + c_1\lambda^3 + c_2\lambda^2 + c_3\lambda + c_4),$$

480 where $\lambda_1 = \mu_0(s_0^{\text{in}}, M_2(D + a_2)) - D - a_0$ and the coefficients c_i are given by:

$$481 \quad c_1 = 2D + (G + H)x_1 + Ix_2,$$

$$482 \quad c_2 = D^2 + (G + H)(D + K)x_1 + I(D + L)x_2 + GIx_1x_2,$$

$$483 \quad c_3 = D(G + H)Kx_1 + DILx_2 + GI(K + L)x_1x_2 \quad \text{and} \quad c_4 = GIKLx_1x_2.$$

485 From Lemma B.1, the roots of the fourth order polynomial are of negative real parts
486 if and only if

$$487 \quad \text{(C.10)} \quad c_i > 0, \quad \text{for } i = 1, 3, 4 \quad \text{and} \quad r_1 = c_1c_2c_3 - c_1^2c_4 - c_3^2 > 0.$$

489 We always have $c_i > 0$, for $i = 1, 3, 4$. We can write r_1 as follows:

$$490 \quad \begin{aligned} r_1 = &DK [(D + K)(G + H)^3 - G^3K] x_1^3 + D^2I^3Lx_2^3 + G^2I^2(G + H)(K + L)x_1^3x_2^2 + G^2I^3(K + L)x_1^2x_2^3 \\ &+ GI [D(2K + L)(G + H)^2 + HK^2(2G + H)] x_1^3x_2 + DGI^3(K + 2L)x_1x_2^3 + 3D^3I^2Lx_2^2 \\ &+ D^2K [3D(G + H)^2 + HK(2G + H)] x_1^2 + GI^2 [D(K + L)(5G + 3H) + H(K^2 + L^2)] x_1^2x_2^2 \\ &+ DI [H(DH(2K + L) + HK(K + 2L) + DG(9K + 5L) + 2GK^2) + DG^2(7K + 4L)] x_1^2x_2 \\ &+ DI^2 [DG(4K + 7L) + HL(2K + L) + DH(K + 2L)] x_1x_2^2 + 2D^4K(G + H)x_1 + 2D^4ILx_2 \\ &+ D^2I [D(K + L)(5G + 3H) + 2HKL] x_1x_2 + (D^2 + DGx_1 + DIx_2 + GIx_1x_2) (GKx_1 - ILx_2)^2. \end{aligned}$$

491 Thus, $r_1 > 0$. Consequently, the conditions (C.10) are satisfied. Finally, SS8 is stable
492 if and only if $\lambda_1 < 0$, that is to say $\mu_0(s_0^{\text{in}}, M_2(D + a_2)) < D + a_0$. Since M_0 is
493 increasing, this condition is equivalent to the stability condition of SS8 in Table 3.

494 **C.2. Proof of Proposition 3.3.** If SS2 exists then, its condition of existence
495 $\mu_2(s_2^{\text{in}}) > D + a_2$ holds. Therefore, the condition $\mu_2(s_2^{\text{in}}) < D + a_2$ of stability of
496 SS1 is not satisfied.

497 If SS3 exists then, its condition of existence $\mu_0(s_0^{\text{in}}, s_2^{\text{in}}) > D + a_0$ holds. Therefore,
498 the condition $\mu_0(s_0^{\text{in}}, s_2^{\text{in}}) < D + a_0$ of stability of SS1 is not satisfied.

499 If SS7 exists then, its condition of existence $\mu_1(s_1^{\text{in}}, s_2^{\text{in}}) > D + a_1$ holds. Therefore,
500 the condition $\mu_1(s_1^{\text{in}}, s_2^{\text{in}}) < D + a_1$ of stability of SS1 is not satisfied.

501 If SS6 exists then, the conditions

$$502 \quad (1 - \omega)s_0^{\text{in}} + s_1^{\text{in}} + s_2^{\text{in}} > \phi_2(D), \quad s_0^{\text{in}} > \varphi_0(D), \quad s_0^{\text{in}} + s_1^{\text{in}} > \varphi_0(D) + \varphi_1(D)$$

503 hold. Therefore, the condition $s_0^{\text{in}} < \varphi_0(D)$ of stability of SS2 or SS8 is not satisfied,
 504 the condition $(1 - \omega)s_0^{\text{in}} + s_1^{\text{in}} + s_2^{\text{in}} < \phi_2(D)$ of stability of SS4 is not satisfied, and
 505 the condition $s_0^{\text{in}} + s_1^{\text{in}} < \varphi_0(D) + \varphi_1(D)$ of stability of SS5 is not satisfied.
 506 If SS5 exists then, its conditions of existence

$$507 \quad s_0^{\text{in}} > \varphi_0(D) \quad \text{and} \quad s_2^{\text{in}} - \omega s_0^{\text{in}} > M_2(D + a_2) - \omega \varphi_0(D)$$

508 hold. Therefore, the condition $s_0^{\text{in}} < \varphi_0(D)$ of stability of SS2 or SS8 is not satisfied
 509 and the condition $s_2^{\text{in}} - \omega s_0^{\text{in}} < M_2(D + a_2) - \omega \varphi_0(D)$ of stability of SS3 is not satisfied.
 510 If SS8 exists then, its conditions of existence $s_1^{\text{in}} + s_2^{\text{in}} > \varphi_1(D) + M_2(D + a_2)$
 511 holds. Therefore, the condition $s_1^{\text{in}} + s_2^{\text{in}} < \varphi_1(D) + M_2(D + a_2)$ of stability of SS7 is
 512 not satisfied.

513 **Appendix D. Proof of Proposition 4.1.** We assume that the biological
 514 parameter values in model (4.2) are provided in Table 15. We assume that $S_{\text{ph}}^{\text{in}} = 0$,
 515 $S_{\text{H}_2}^{\text{in}} = 2.67 \times 10^{-5}$ as in Fig. 3(a) of [26]. We assume that $S_{\text{ch}}^{\text{in}} = 0.1$. As said in
 516 Section 4, Theorem 3.1 applies to model (4.2). Using the change of variables (G.2)
 517 and Table 3, SS7 and SS8 do not exist when $S_{\text{ph}}^{\text{in}} = 0$. Moreover, the necessary and
 518 sufficient existence and stability conditions of steady states of (4.2) are summarized
 in Table 9.

TABLE 9

Existence and local stability conditions of steady states of (4.2), when $S_{\text{ph}}^{\text{in}} = 0$. The functions μ_i are given in (G.3) while c_3, c_5, r_4 and r_5 are defined in Table 2. All other functions are given in Table 8 and Table 16.

	Existence conditions	Stability conditions
SS1	Always exists	$\mu_0(Y S_{\text{ch}}^{\text{in}}, S_{\text{H}_2}^{\text{in}}) < D + a_0, \mu_2(S_{\text{H}_2}^{\text{in}}) < D + a_2$
SS2	$\mu_2(S_{\text{H}_2}^{\text{in}}) > D + a_2$	$Y S_{\text{ch}}^{\text{in}} < \varphi_0(D)$
SS3	$\mu_0(Y S_{\text{ch}}^{\text{in}}, S_{\text{H}_2}^{\text{in}}) > D + a_0$	$\mu_1(Y S_{\text{ch}}^{\text{in}} - s_0, S_{\text{H}_2}^{\text{in}} - \omega(Y S_{\text{ch}}^{\text{in}} - s_0)) < D + a_1$ $S_{\text{H}_2}^{\text{in}} - \omega Y S_{\text{ch}}^{\text{in}} < M_2(D + a_2) - \omega \varphi_0(D)$ with s_0 solution of $\psi_0(s_0) = D + a_0$
SS4	$(1 - \omega)Y S_{\text{ch}}^{\text{in}} + S_{\text{H}_2}^{\text{in}} \geq \phi_1(D)$, $Y S_{\text{ch}}^{\text{in}} > M_0(D + a_0, s_2) + M_1(D + a_1, s_2)$ with s_2 solution of $\Psi(s_2, D) = (1 - \omega)Y S_{\text{ch}}^{\text{in}} + S_{\text{H}_2}^{\text{in}}$	$(1 - \omega)Y S_{\text{ch}}^{\text{in}} + S_{\text{H}_2}^{\text{in}} < \phi_2(D), \phi_3(D) > 0$ $\frac{\partial \Psi}{\partial s_2}(s_2, D) > 0$
SS5	$Y S_{\text{ch}}^{\text{in}} > \varphi_0(D)$, $S_{\text{H}_2}^{\text{in}} - \omega Y S_{\text{ch}}^{\text{in}} > M_2(D + a_2) - \omega \varphi_0(D)$	$Y S_{\text{ch}}^{\text{in}} < \varphi_0(D) + \varphi_1(D)$
SS6	$(1 - \omega)Y S_{\text{ch}}^{\text{in}} + S_{\text{H}_2}^{\text{in}} > \phi_2(D)$, $Y S_{\text{ch}}^{\text{in}} > \varphi_0(D) + \varphi_1(D)$	$c_3 > 0, c_5 > 0, r_4 > 0, r_5 > 0$

519

520 SS1 always exists and it is stable if and only if

$$521 \quad D > \mu_0(Y S_{\text{ch}}^{\text{in}}, S_{\text{H}_2}^{\text{in}}) - a_0 := \delta_6 \quad \text{and} \quad D > \mu_2(S_{\text{H}_2}^{\text{in}}) - a_2 := \delta_7.$$

Thus, SS1 is stable if and only if $D > \max(\delta_6, \delta_7) = \delta_7$ (see Table 4 for all critical parameter values $\delta_i, i = 1, \dots, 7$). From Table 9, SS2 exists if and only if $D < \delta_7$. From the eigenvalues λ_1 and λ_2 defined by (C.1), we deduce that SS2 is stable if and only if

$$F_1(D) := \mu_0(Y S_{\text{ch}}^{\text{in}}, M_2(D + a_2)) - D - a_0 < 0 \quad \iff \quad \delta_5 < D < \delta_7$$

522 where δ_5 is the solution of equation $F_1(D) = 0$ (see Figure D.1). SS3 exists if and

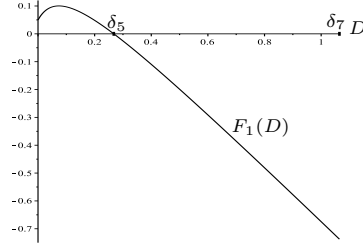


FIG. D.1. Stability of SS2 for all $D \in (\delta_5, \delta_7)$: change of sign of the function $F_1(D)$.

523 only if $D < \delta_6$ and it is stable if and only if

524
$$F_2(D) := \mu_1 (S_{\text{ch}}^{\text{in}} Y - s_0, S_{\text{H}_2}^{\text{in}} - \omega (S_{\text{ch}}^{\text{in}} Y - s_0)) - D - a_1 < 0,$$

525
$$F_3(D) := S_{\text{H}_2}^{\text{in}} + \omega (\varphi_0(D) - Y S_{\text{ch}}^{\text{in}}) - M_2(D + a_2) < 0,$$

that is, $D < \delta_4$, where δ_4 is the solution of equation $F_3(D) = 0$ (see Figure D.2). From Remark 3.2, the system can have at most two steady states of the form SS4

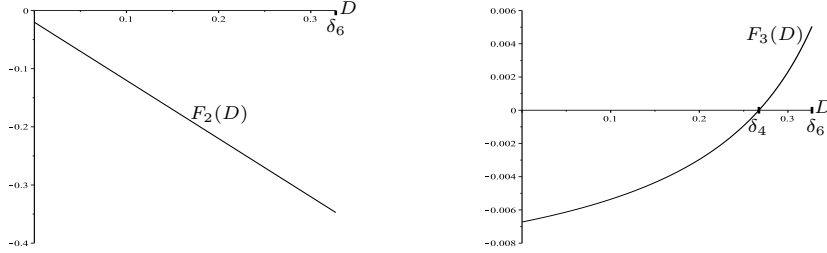


FIG. D.2. Stability of SS3 for all $D < \delta_4$: signs of the functions $F_2(D)$ and $F_3(D)$.

denoted by SS4¹ and SS4² as $\omega \simeq 0.53 < 1$. Their first existence condition in Table 9 holds if and only if

$$F_4(D) := \phi_1(D) - S_{\text{H}_2}^{\text{in}} - (1 - \omega)Y S_{\text{ch}}^{\text{in}} \leq 0 \iff D \leq \delta_3$$

where δ_3 is the solution of equation $F_4(D) = 0$ (see Figure D.3(a)). Their second existence condition holds for all $D \leq \delta_3$, since the straight line of equation $y = Y S_{\text{ch}}^{\text{in}}$ is above the curve of the function $y = M_0(D + a_0, s_2^{*i}) + M_1(D + a_1, s_2^{*i})$, for $i = 1, 2$, which correspond to SS4¹ and SS4², respectively, (see Figure D.3(b)). From

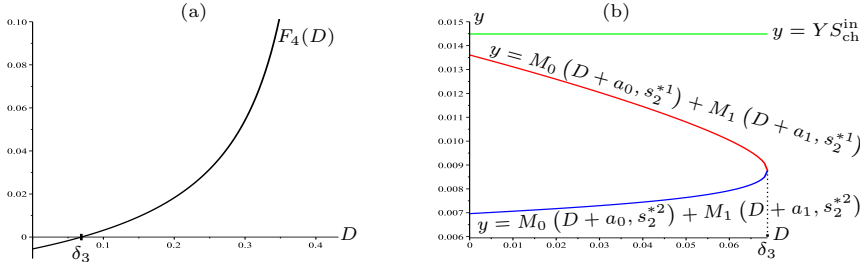


FIG. D.3. Existence of SS4 for all $D \leq \delta_3$: (a) change of sign of the function $F_4(D)$, (b) the green line of equation $y = Y S_{\text{ch}}^{\text{in}}$ is above the red and blue curves of the functions $M_0(D + a_0, s_2^{*i}) + M_1(D + a_1, s_2^{*i})$, $i = 1, 2$, respectively.

Remark 3.2 and Table 9, SS4¹ is unstable for all $0 < D < \delta_3$ while SS4² is stable if

and only if

$$F_5(D) := \phi_2(D) - S_{H_2}^{\text{in}} - (1 - \omega)Y S_{\text{ch}}^{\text{in}} > 0 \quad \text{and} \quad \phi_3(D) > 0,$$

526 that is, $D \in (\delta_2, \delta_3)$ where δ_2 is the solution of equation $F_5(D) = 0$ (see [Figure D.4](#)).
 527 Indeed, $F_5(D) > 0$ for all $D \in (\delta_2, \delta_3)$ and $\phi_3(D) > 0$ for all $D \in (\delta'_2, \delta_3)$ where
 $\delta'_2 \simeq 0.057865$ is the solution of equation $\phi_3(D) = 0$ such that $\delta'_2 < \delta_2$.

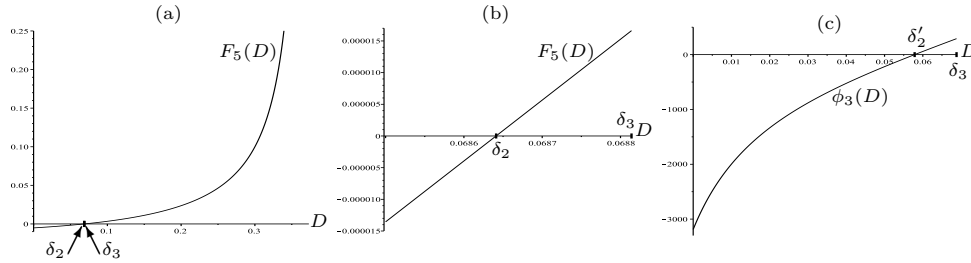


FIG. D.4. Stability of SS_4 for all $D \in (\delta_2, \delta_3)$: (a) Curve of the function $F_5(D)$. (b) Magnification of $F_5(D)$ for $D \in [0.0685, 0.0688]$. (c) Curve of the function $\phi_3(D)$.

528

SS_5 exists if and only if $F_1(D) > 0$ and $F_3(D) > 0$, that is, $\delta_4 < D < \delta_5$. SS_5 is stable if and only if

$$F_6(D) := \varphi_0(D) + \varphi_1(D) - Y S_{\text{ch}}^{\text{in}} > 0,$$

that is, for all $D \in (\delta_4, \delta_5)$ (see [Figure D.5](#)).

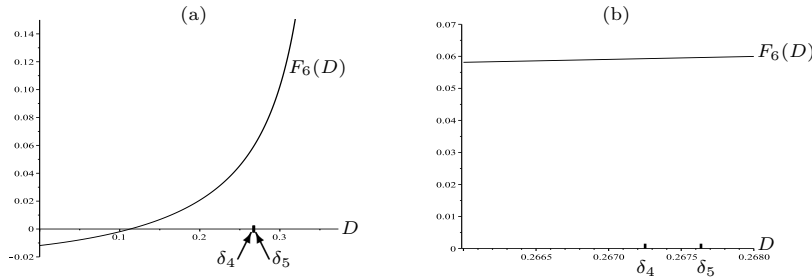


FIG. D.5. Stability of SS_5 for all $D \in (\delta_4, \delta_5)$ and existence of SS_6 for all $D < \delta_2$: (a) curve of the function $F_6(D)$. (b) Magnification of $F_6(D)$ for $D \in [0.266, 0.268]$.

529

530

531

532

533

534

535

536

SS_6 exists if and only if $F_5(D) < 0$ and $F_6(D) < 0$, that is, for all $D < \delta_2$ where δ_2 is the solution of the equation $F_5(D) = 0$ (see [Figure D.4\(a-b\)](#) and [Figure D.5](#)).
 Indeed, $F_5(D) < 0$ for all $D < \delta_2$ and $F_6(D) < 0$ for all $D < \delta''_2$ where $\delta''_2 \simeq 0.113033$ is the solution of equation $F_6(D) = 0$ such that $\delta_2 < \delta''_2$. To determine the stability of SS_6 , the functions c_3 , c_5 , r_4 and r_5 are plotted with respect to $D < \delta_2$. [Figure D.6](#) shows that $c_3(D)$, $c_5(D)$, $r_4(D)$ and $r_5(D)$ are all positive if and only if $\delta_1 < D < \delta_2$ where $\delta_1 \simeq 0.010412$ is the solution of equation $r_5(D) = 0$.

To give a numerical evidence of the Hopf bifurcation occurring for $D = \delta_1$, we determine numerically the eigenvalues of the Jacobian matrix of system (4.2) at SS_6 and we plot them with respect to D . [Figure D.7\(a-b\)](#) shows that two eigenvalues denoted by $\lambda_1(D)$ and $\lambda_2(D)$ are real and remain negative for all $D \in [0, \delta_2]$. [Figure D.7\(c\)](#) shows that the two other eigenvalues $\lambda_3(D)$ and $\lambda_4(D)$ form a complex-conjugate pair denoted by

$$\lambda_{3,4}(D) = \alpha_{3,4}(D) \pm i\beta_{3,4}(D), \quad \text{for all } D \in [0, \delta^*),$$

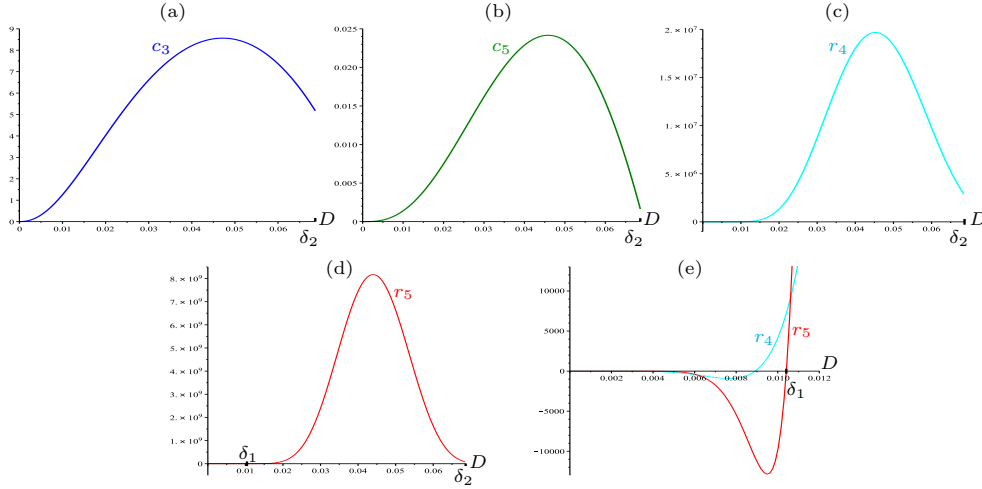


FIG. D.6. (a-b-c-d) Curves of the functions $c_3(D)$, $c_5(D)$, $r_4(D)$ and $r_5(D)$ for $0 < D < \delta_2$. (e) Magnification of the curve of r_4 and r_5 for $D \in [0, 0.02]$.

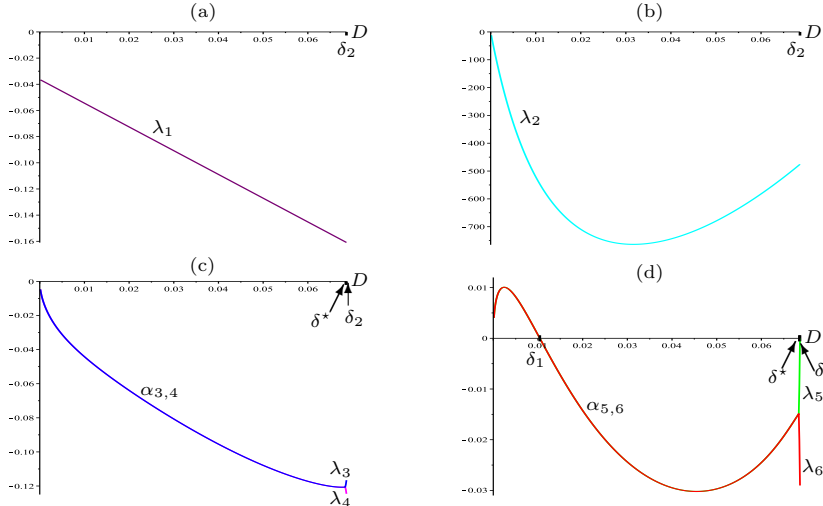


FIG. D.7. The eigenvalues of the Jacobian matrix at SS6 as a function of D , when $S_{\text{ch}}^{\text{in}} = 0.1$, $S_{\text{ph}}^{\text{in}} = 0$ and $S_{\text{H}_2}^{\text{in}} = 2.67 \times 10^{-5}$. (c-d) The real parts $\alpha_{3,4}$ and $\alpha_{5,6}$ for $D \in [0, \delta^*]$.

where the real part $\alpha_{3,4}$ remains negative and $\delta^* \simeq 0.068504$. Then, they become real, negative and distinct for all $D \in (\delta^*, \delta_2)$. Similarly, Figure D.7(d) shows that the two last eigenvalues $\lambda_5(D)$ and $\lambda_6(D)$ form a complex-conjugate pair denoted by

$$\lambda_{5,6}(D) = \alpha_{5,6}(D) \pm i\beta_{5,6}(D), \quad \text{for all } D \in [0, \delta^*),$$

where the real part $\alpha_{5,6}$ is positive for all $D \in [0, \delta_1)$ and negative for all $D \in (\delta_1, \delta^*)$. Then, for all $D \in (\delta^*, \delta_2)$, they become real, negative and distinct. At the particular value $D = \delta_1$, the pair $\lambda_{5,6}(D)$ is purely imaginary such that $\alpha_{5,6}(\delta_1) = 0$, with $\beta_{5,6}(\delta_1) \neq 0$. Moreover, one has

$$\frac{d\alpha_{5,6}}{dD}(\delta_1) < 0.$$

537 This is consistent with Figure 4.1(b) showing that, as D decreases and crosses δ_1 ,
 538 the steady state SS6 becomes unstable and we have a supercritical Hopf bifurcation,

539 leading to the appearance, from the steady state SS6, of small-amplitude periodic
540 oscillations.

541 **Appendix E. Bifurcation diagram with respect to $S_{\text{ch}}^{\text{in}}$.** In the following,
542 we consider $S_{\text{ph}}^{\text{in}} = 0$ and $S_{\text{H}_2}^{\text{in}} = 2.67 \times 10^{-5}$, corresponding to Fig. 3(a) in [26] and
543 we fix $D = 0.01$. Then, we determine the bifurcation diagram, where the input con-
544 centration $S_{\text{ch}}^{\text{in}}$ is the bifurcation parameter. This choice for the operating parameters
545 is identical to that in [16] excepted that we have added the microbial decay terms,
546 as in [26]. Our aim is to compare our results to those of [26] and to see if there are
547 interesting phenomena that were not detected in the operating diagram depicted in
548 Fig. 3(a) of [26], see Remark E.2. Our aim is also to see the effects of mortality on the
549 behavior of the process and to compare our bifurcation diagram to the one depicted in
550 [16], see Remark E.3 below. Using Theorem 3.1, we have the following result, which
551 is supported by numerical experimentation and is proved in Appendix F.

552 *Proposition E.1.* Let $S_{\text{ph}}^{\text{in}} = 0$, $S_{\text{H}_2}^{\text{in}} = 2.67 \times 10^{-5}$ and $D = 0.01$. In this case,
553 SS7 and SS8 do not exist. Using the biological parameter values in Table 15, the
554 bifurcation values σ_i , $i = 1, \dots, 6$ are provided in Table 10. The bifurcation analysis
555 of (4.2) according to $S_{\text{ch}}^{\text{in}}$ is given in Table 11. The bifurcation types at the critical
556 values σ_i are defined in Table 12.

TABLE 10

Critical parameter values σ_i , for $i = 1, \dots, 6$ where Y is defined in Appendix G, r_5 in Table 2 while all other functions are given in Table 8. Note that $\sigma_1 < \sigma_3 < \sigma_4 < \sigma_2 < \sigma_5 < \sigma_6$, compare with Table 5 in [16].

Definition	Value
$\sigma_1 = M_0 (D + a_0, S_{\text{H}_2}^{\text{in}}) / Y$	0.003173
$\sigma_2 = (\phi_1(D) - S_{\text{H}_2}^{\text{in}}) / ((1 - \omega)Y)$	0.029402
$\sigma_3 = \varphi_0(D) / Y$	0.013643
$\sigma_4 = (S_{\text{H}_2}^{\text{in}} - M_2(D + a_2) + \omega\varphi_0(D)) / (\omega Y)$	0.013985
$\sigma_5 = (\phi_2(D) - S_{\text{H}_2}^{\text{in}}) / ((1 - \omega)Y)$	0.033292
σ_6 is the largest root of equation $r_5 = 0$	0.1025

TABLE 11

Existence and stability of steady states, with respect to $S_{\text{ch}}^{\text{in}}$. The bifurcation values σ_i , $i = 1, \dots, 6$ are given in Table 10.

Interval	SS1	SS2	SS3	SS4 ¹	SS4 ²	SS5	SS6
$0 < S_{\text{ch}}^{\text{in}} < \sigma_1$	U	S					
$\sigma_1 < S_{\text{ch}}^{\text{in}} < \sigma_3$	U	S	U				
$\sigma_3 < S_{\text{ch}}^{\text{in}} < \sigma_4$	U	U	U			S	
$\sigma_4 < S_{\text{ch}}^{\text{in}} < \sigma_2$	U	U	S	U	U		
$\sigma_2 < S_{\text{ch}}^{\text{in}} < \sigma_5$	U	U	S	U	U		U
$\sigma_5 < S_{\text{ch}}^{\text{in}} < \sigma_6$	U	U	S	U	U		U
$\sigma_6 < S_{\text{ch}}^{\text{in}}$	U	U	S	U	U		S

557 *Remark E.2.* As explained in Remark 4.2, the operating diagram of Fig. 3(a) in
558 [26] for $D = 0.01$ does not accurately describe the transition from the region labeled
559 SS2 (corresponding to the stability of SS2) to the SS3 region (corresponding to the
560 stability of SS3). Our results show that this transition is via a SS5 region, which is very
561 thin, since it corresponds to $\sigma_3 < S_{\text{ch}}^{\text{in}} < \sigma_4$, where $\sigma_3 \simeq 0.013643$ and $\sigma_4 \simeq 0.013985$.

TABLE 12

Bifurcation types corresponding to the critical values of σ_i , $i = 1, \dots, 6$, defined in Table 10. There exists also a critical value $\sigma^* \simeq 0.099295 \in (\sigma_5, \sigma_6)$ corresponding to the value of $S_{\text{ch}}^{\text{in}}$ where the stable limit cycle disappears when $S_{\text{ch}}^{\text{in}}$ is decreasing.

Bifurcation types	
σ_1	Transcritical bifurcation of SS1 and SS3
σ_2	Saddle-node bifurcation of SS4 ¹ and SS4 ²
σ_3	Transcritical bifurcation of SS2 and SS5
σ_4	Transcritical bifurcation of SS3 and SS5
σ_5	Transcritical bifurcation of SS4 ¹ and SS6
σ_6	Supercritical Hopf bifurcation
σ^*	Disappearance of the stable limit cycle

562 This region was missing in Fig. 3(a) in [26], since $\sigma_4 - \sigma_3$ is of order 10^{-4} . Indeed,
 563 the limitations of the operating diagram in Fig. 3(a) in [26] are due to the numerical
 564 resolution: the stability of SS5 occurs in a very small region and may not be detected
 565 if the step size was for example an order of magnitude greater than $\sigma_4 - \sigma_3$.

566 Figures E.1 and E.2 show the one-parameter bifurcation diagrams of X_{ch} and
 567 X_{H_2} versus $S_{\text{ch}}^{\text{in}}$ in system (4.2), respectively. The magnifications of the bifurcation
 568 diagrams are illustrated in Figure E.1(b), Figure E.2(b) and Figure E.3 showing the
 569 transcritical bifurcations at σ_1 , σ_3 , σ_4 and σ_5 , the saddle-node bifurcation at σ_2 , the
 570 Hopf bifurcation at σ_6 and the disappearance of the cycle at σ^* . In Figure E.1(b),
 571 SS1 and SS2 cannot be distinguished since they have both a zero X_{ch} -component. As
 572 SS2 is stable and SS1 is unstable for $S_{\text{ch}}^{\text{in}} < \sigma_3$, the $X_{\text{ch}} = 0$ axis is plotted in blue as
 573 the color of SS2 in Table 7. In Figure E.2(b), SS1 and SS2 are distinguished but it is
 574 not the case for SS1 and SS3, since they have both a zero X_{H_2} -component. As SS3 is
 575 stable and SS1 is unstable for $S_{\text{ch}}^{\text{in}} > \sigma_4$, the $X_{\text{H}_2} = 0$ axis is plotted in purple as the
 color of SS3 in Table 7.

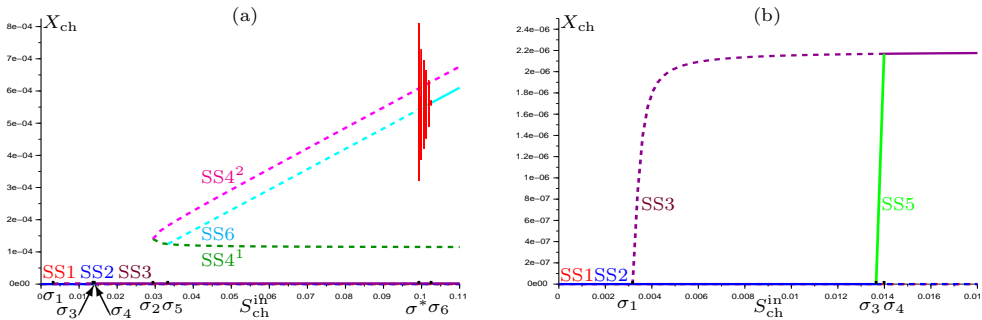


FIG. E.1. (a) Bifurcation diagram of X_{ch} versus $S_{\text{ch}}^{\text{in}} \in [0, 0.11]$ in model (4.2) showing the appearance and disappearance of stable limit cycles. (b) Magnification on the transcritical bifurcations for $S_{\text{ch}}^{\text{in}} \in [0, 0.018]$.

576

577 Remark E.3. As explained in Remark 3.2, with the exception of SS6, the main-
 578 tenance does not destabilize the steady states. Only their regions of existence and
 579 stability, with respect to the operating parameters, can be modified. For SS6, it is
 580 more difficult to answer the question of whether or not it can be destabilized by in-
 581 cluding maintenance terms. The bifurcations diagrams depicted in Figures E.1 to E.3,
 582 and the results given in Proposition E.1, permit to answer this question at least for
 583 the following values of the operating parameters $S_{\text{ph}}^{\text{in}} = 0$, $S_{\text{H}_2}^{\text{in}} = 2.67 \times 10^{-5}$, $D = 0.01$

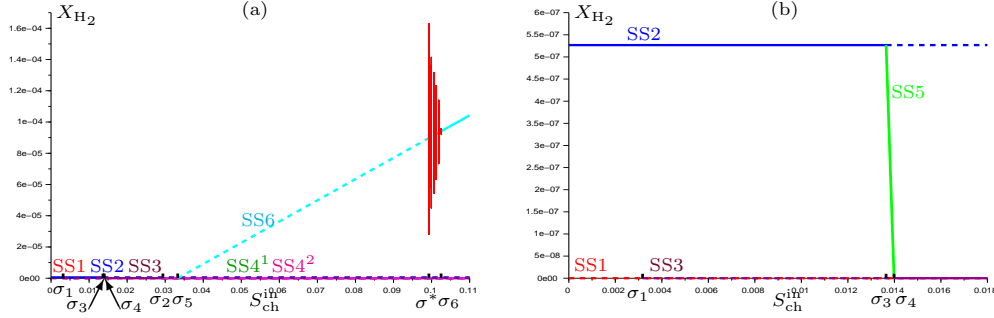


FIG. E.2. (a) Bifurcation diagram of X_{H_2} versus $S_{ch}^{in} \in [0, 0.11]$ in model (4.2). (b) Magnification on the transcritical bifurcations for $S_{ch}^{in} \in [0, 0.018]$.

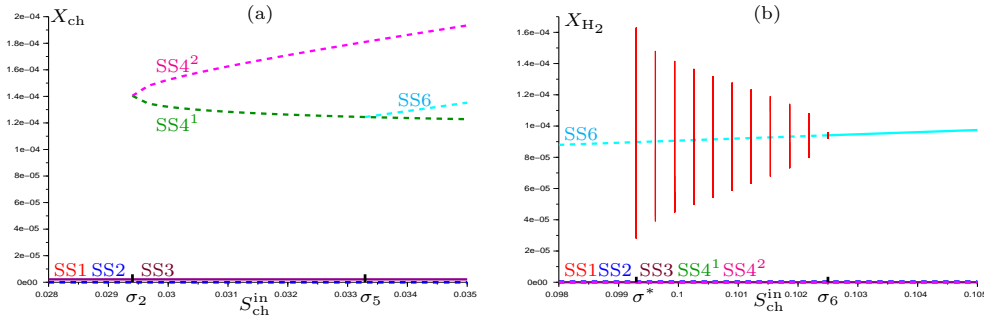


FIG. E.3. (a) Magnification on the saddle-node bifurcation at $S_{ch}^{in} = \sigma_2$ and the transcritical bifurcation at $S_{ch}^{in} = \sigma_5$ for $S_{ch}^{in} \in [0.028, 0.035]$. (b) Magnification on the limit cycles for $S_{ch}^{in} \in [0.098, 0.105]$.

584 and $S_{ch}^{in} \geq 0$. The comparison of the results obtained in Table 11 with those given
 585 in Table 6 of [16] shows only minor changes in the bifurcation values σ_i , $i = 1, \dots, 6$.
 586 Therefore, even for SS6, the maintenance does not destabilize the system: only the
 587 regions of stability, with respect to the operating parameters, are slightly modified.
 588 Note that the change of the bifurcation values σ_i is predictable since their formulas
 589 in Table 10 involve the added decay terms. However, the saddle-node bifurcation at
 590 σ_2 arises after and not before the transcritical bifurcations at σ_3 and σ_4 as in [16].

591 **Appendix F. Proof of Proposition E.1.** As said in Section 4, Theorem 3.1
 592 applies to model (4.2). From Theorem 3.1 and the change of variables (G.2), SS7 and
 593 SS8 do not exist since $S_{ph}^{in} = 0$. The necessary and sufficient existence and stability
 594 conditions of all other steady states are summarized in Table 9. Since the second
 595 stability condition of SS1 in Table 9 does not hold

$$596 \quad (F.1) \quad \mu_2(S_{H_2}^{in}) \simeq 1.0845 > D + a_2 = 0.03,$$

SS1 always exists and is unstable. Since the existence condition of SS2 in Table 9
 holds (see inequality (F.1)), SS2 exists and is stable if and only if

$$S_{ch}^{in} < \varphi_0(D)/Y =: \sigma_3.$$

SS3 exists if and only if

$$S_{ch}^{in} > M_0(D + a_0, S_{H_2}^{in})/Y =: \sigma_1.$$

598 Let $F(S_{\text{ch}}^{\text{in}})$ be the function defined by

600 (F.2)
$$F(S_{\text{ch}}^{\text{in}}) = \mu_1 (S_{\text{ch}}^{\text{in}} Y - s_0, S_{\text{H}_2}^{\text{in}} - \omega (S_{\text{ch}}^{\text{in}} Y - s_0)).$$

The first stability condition of SS3 in Table 9 holds for all $S_{\text{ch}}^{\text{in}} > \sigma_1$, that is, $F(S_{\text{ch}}^{\text{in}}) < D + a_1$ since the maximum of F is smaller than 0.0013 while $D + a_1 = 0.03$ (see Figure F.1). From the second stability condition in Table 9, SS3 is stable if and only if

$$S_{\text{ch}}^{\text{in}} > (S_{\text{H}_2}^{\text{in}} - M_2(D + a_2) + \omega\varphi_0(D)) / (\omega Y) =: \sigma_4.$$

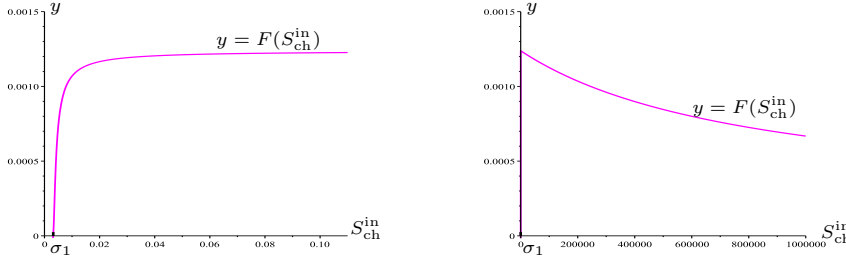


FIG. F.1. Curve of the function $y = F(S_{\text{ch}}^{\text{in}})$ defined by (F.2).

601

From Theorem 3.1, the system can have at most two steady states of the form SS4 denoted by SS4^1 and SS4^2 as $\omega \simeq 0.53 < 1$. Their first existence condition in Table 9 holds if and only if

$$S_{\text{ch}}^{\text{in}} \geq (\phi_1(D) - S_{\text{H}_2}^{\text{in}}) / ((1 - \omega)Y) =: \sigma_2.$$

602 Their second existence condition holds, for all $S_{\text{ch}}^{\text{in}} \in [\sigma_2, 0.11]$, since the straight line
 603 of equation $y = S_{\text{ch}}^{\text{in}} Y$ is above the curves of the functions $y = M_0(D + a_0, s_2^{*i}) +$
 604 $M_1(D + a_1, s_2^{*i})$, for $i = 1, 2$, respectively (see Figure F.2). Thus, SS4^1 and SS4^2
 605 exist and are unstable for all $S_{\text{ch}}^{\text{in}} > \sigma_2$ since the second stability condition does not
 hold where $\phi_3(D) \simeq -1996.917 < 0$.

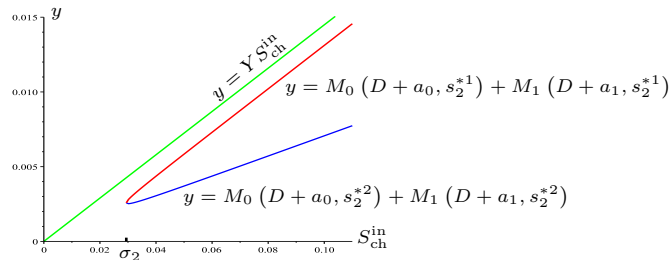


FIG. F.2. The green line of equation $y = Y S_{\text{ch}}^{\text{in}}$ is above the red and blue curves of the functions $M_0(D + a_0, s_2^{*i}) + M_1(D + a_1, s_2^{*i})$, for $i = 1, 2$, which correspond to SS4^1 and SS4^2 , respectively.

606

SS5 exists if and only if $\sigma_3 := \varphi_0(D)/Y < S_{\text{ch}}^{\text{in}} < \sigma_4$. When it exists, SS5 is stable since

$$S_{\text{ch}}^{\text{in}} < \sigma_4 \simeq 0.013985 < (\varphi_0(D) + \varphi_1(D))/Y \simeq 0.02304.$$

SS6 exists if and only if

$$S_{\text{ch}}^{\text{in}} > \frac{\phi_2(D) - S_{\text{H}_2}^{\text{in}}}{(1 - \omega)Y} =: \sigma_5 \simeq 0.033292, \quad S_{\text{ch}}^{\text{in}} > \frac{\varphi_0(D) + \varphi_1(D)}{Y} \simeq 0.02304.$$

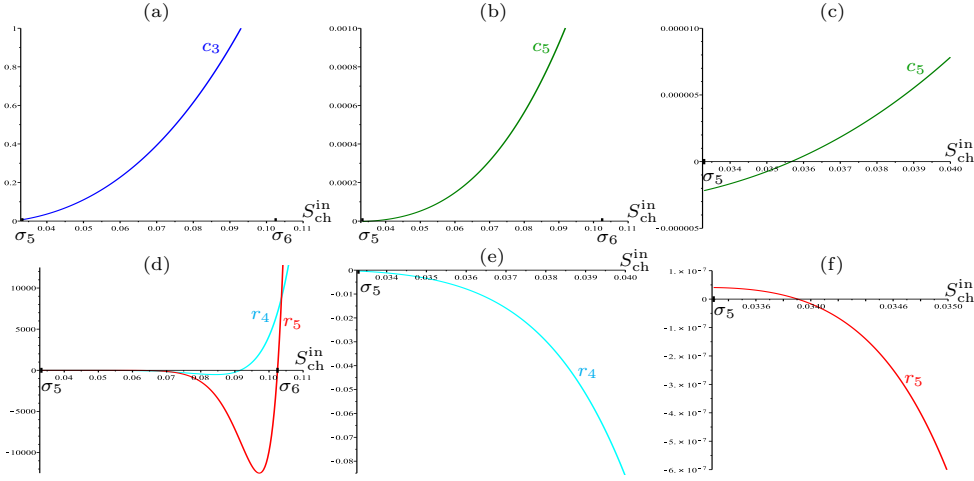


FIG. F.3. (a-b-d) Curves of the functions $c_3(S_{\text{ch}}^{\text{in}})$, $c_5(S_{\text{ch}}^{\text{in}})$, $r_4(S_{\text{ch}}^{\text{in}})$ and $r_5(S_{\text{ch}}^{\text{in}})$ for $S_{\text{ch}}^{\text{in}} > \sigma_5$. (c-e-f) Magnifications of the curves c_5 and r_4 for $S_{\text{ch}}^{\text{in}} \in [\sigma_5, 0.04]$ and of r_5 for $S_{\text{ch}}^{\text{in}} \in [\sigma_5, 0.035]$.

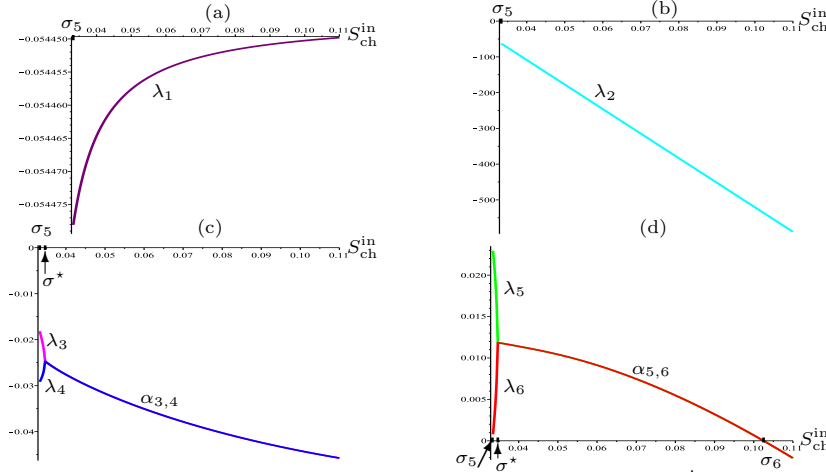


FIG. F.4. The eigenvalues of the Jacobian matrix at SS6 as a function of $S_{\text{ch}}^{\text{in}}$, when $D = 0.01$, $S_{\text{ph}}^{\text{in}} = 0$ and $S_{\text{H}_2}^{\text{in}} = 2.67 \times 10^{-5}$. (c-d) The real parts $\alpha_{3,4}$ and $\alpha_{5,6}$ for $S_{\text{ch}}^{\text{in}} \in (\sigma^*, 0.11]$.

Hence, SS6 exists if and only if $S_{\text{ch}}^{\text{in}} > \sigma_5$. To determine the stability of SS6, the functions c_3 , c_5 , r_4 and r_5 are plotted with respect to $S_{\text{ch}}^{\text{in}} > \sigma_5$. Figure F.3 shows that $c_3(S_{\text{ch}}^{\text{in}})$, $c_5(S_{\text{ch}}^{\text{in}})$, $r_4(S_{\text{ch}}^{\text{in}})$ and $r_5(S_{\text{ch}}^{\text{in}})$ are all positive if and only if $S_{\text{ch}}^{\text{in}} > \sigma_6$ where $\sigma_6 \simeq 0.1025$ is the largest root of equation $r_5(S_{\text{ch}}^{\text{in}}) = 0$. To give a numerical evidence of the Hopf bifurcation occurring for $S_{\text{ch}}^{\text{in}} = \sigma_6$, we determine numerically the eigenvalues of the Jacobian matrix of system (4.2) at SS6 and we plot them with respect to $S_{\text{ch}}^{\text{in}}$. Figure F.4(a-b) shows that two eigenvalues denoted by $\lambda_1(S_{\text{ch}}^{\text{in}})$ and $\lambda_2(S_{\text{ch}}^{\text{in}})$ are real and remain negative for all $S_{\text{ch}}^{\text{in}} \in (\sigma_5, 0.11]$. Figure F.4(c) shows that the two other eigenvalues $\lambda_3(S_{\text{ch}}^{\text{in}})$ and $\lambda_4(S_{\text{ch}}^{\text{in}})$ are real, negative and distinct for all $S_{\text{ch}}^{\text{in}} \in (\sigma_5, \sigma^*)$ where $\sigma^* \simeq 0.03467$. Then, they become a complex-conjugate pair denoted by

$$\lambda_{3,4}(S_{\text{ch}}^{\text{in}}) = \alpha_{3,4}(S_{\text{ch}}^{\text{in}}) \pm i\beta_{3,4}(S_{\text{ch}}^{\text{in}}), \quad \text{for all } S_{\text{ch}}^{\text{in}} \in (\sigma^*, 0.11]$$

607 where the real part $\alpha_{3,4}$ remains negative.

Figure F.4(d) shows that the two last eigenvalues $\lambda_5(S_{\text{ch}}^{\text{in}})$ and $\lambda_6(S_{\text{ch}}^{\text{in}})$ are real, positive and distinct for all $S_{\text{ch}}^{\text{in}} \in (\sigma_5, \sigma^*]$. Then, they become a complex-conjugate pair denoted by

$$\lambda_{5,6}(S_{\text{ch}}^{\text{in}}) = \alpha_{5,6}(S_{\text{ch}}^{\text{in}}) \pm i\beta_{5,6}(S_{\text{ch}}^{\text{in}}), \quad \text{for all } S_{\text{ch}}^{\text{in}} \in (\sigma^*, 0.11],$$

so that the real part $\alpha_{5,6}$ is positive for all $S_{\text{ch}}^{\text{in}} \in (\sigma^*, \sigma_6)$ and negative for all $S_{\text{ch}}^{\text{in}} \in (\sigma_6, 0.11]$. At the particular value $S_{\text{ch}}^{\text{in}} = \sigma_6$, the pair $\lambda_{5,6}(S_{\text{ch}}^{\text{in}})$ is purely imaginary such that $\alpha_{5,6}(\sigma_6) = 0$, with $\beta_{5,6}(\sigma_6) \neq 0$. Moreover, one has

$$\frac{d\alpha_{5,6}}{dS_{\text{ch}}^{\text{in}}}(\sigma_6) < 0.$$

This is consistent with Figures E.1 to E.3, showing that, as $S_{\text{ch}}^{\text{in}}$ decreases and crosses σ_6 , the steady state SS6 changes its stability through a supercritical Hopf bifurcation with the emergence of a stable limit cycle that we illustrate in Figures 4.3 and H.1.

Remark F.1. Note that Figures F.1 and F.2 showing the stability of SS3 and the existence of two steady states of type SS4 are similar to Figures 6 and 7 in [16], respectively. But, on the contrary, Figure F.3 which concerns the stability of SS6 is completely different from Figure 8 in [16], since the conditions of stability of SS6 require to consider the signs of the Liénard-Chipart coefficients c_3 , c_5 , r_4 and r_5 .

Appendix G. A chlorophenol-mineralising three-tiered microbial 'food web'. Following [20], model (4.2) can be written in the form of model (1.1), using the following change of variables:

$$(G.1) \quad x_0 = \frac{Y}{Y_0} X_{\text{ch}}, x_1 = \frac{Y_4}{Y_1} X_{\text{ph}}, x_2 = \frac{1}{Y_2} X_{\text{H}_2}, s_0 = Y S_{\text{ch}}, s_1 = Y_4 S_{\text{ph}}, s_2 = S_{\text{H}_2},$$

where $Y = Y_3 Y_4$. The input concentrations are given by:

$$(G.2) \quad s_0^{\text{in}} = Y S_{\text{ch}}^{\text{in}}, \quad s_1^{\text{in}} = Y_4 S_{\text{ph}}^{\text{in}}, \quad s_2^{\text{in}} = S_{\text{H}_2}^{\text{in}},$$

the death rates are $a_0 = k_{\text{dec, ch}}$, $a_1 = k_{\text{dec, ph}}$, $a_2 = k_{\text{dec, H}_2}$, and the yield coefficients are

$$Y_0 = Y_{\text{ch}}, \quad Y_1 = Y_{\text{ph}}, \quad Y_2 = Y_{\text{H}_2}, \quad Y_3 = 224/208(1 - Y_0), \quad Y_4 = 32/224(1 - Y_1)$$

with $\omega = \frac{16}{208Y} = \frac{1}{2(1-Y_{\text{ch}})(1-Y_{\text{ph}})}$. The specific growth functions (4.1) become the following functions satisfying Hypotheses (H1) to (H8):

$$(G.3) \quad \mu_0(s_0, s_2) = \frac{m_0 s_0}{K_0 + s_0} \frac{s_2}{L_0 + s_2}, \quad \mu_1(s_1, s_2) = \frac{m_1 s_1}{K_1 + s_1} \frac{1}{1 + s_2/K_I}, \quad \mu_2(s_2) = \frac{m_2 s_2}{K_2 + s_2},$$

where

$$\begin{aligned} m_0 &= Y_0 k_{m, \text{ch}}, & K_0 &= Y K_{S, \text{ch}}, & L_0 &= K_{S, \text{H}_2, \text{c}}, & m_1 &= Y_1 k_{m, \text{ph}}, \\ K_1 &= Y_4 K_{S, \text{ph}}, & K_I &= K_{I, \text{H}_2}, & m_2 &= Y_2 k_{m, \text{H}_2}, & K_2 &= K_{S, \text{H}_2}. \end{aligned}$$

For these specific kinetics (G.3), the various functions defined in Table 8 are listed in Table 16. Using the linear change of variable given by (G.1) and (G.2), the yield coefficients in (4.2) are normalized to one except one of them, which is equal to $\omega \simeq 0.53$, when the yield coefficients are those given in Table 15. Therefore, (4.2) is of the form (1.1), with $\omega < 1$ and the results of our paper apply to (4.2).

The aim of this section is to give rigorous proofs for the results of [26] on existence and stability of the steady states of model (4.2). Notice that the results in [26] were

given with respect to the dimensionless form (H.2) of (4.2) by using the variables (H.1) and the growth functions (H.3). The variables (H.1) are related to our variables (G.1) by the formulas

$$x_0 = X_0 K_0, \quad x_1 = X_1 K_1, \quad x_2 = X_2 K_2, \quad s_0 = S_0 K_0, \quad s_1 = S_1 K_1, \quad s_2 = S_2 K_2, \quad t = \tau/m_0.$$

Hence, results given in variables (H.1) can be easily translated into results given in variables (G.1) and vice versa.

From Theorem 3.1, the existence and stability of steady states of model (4.2) can be determine for the specific growth functions (G.3). Using the functions and notations given in Table 16, we have the following results:

SS1 = $(0, 0, 0, s_0^{\text{in}}, s_1^{\text{in}}, s_2^{\text{in}})$ always exists. It is stable if and only if

$$\mu_0(s_0^{\text{in}}, s_2^{\text{in}}) < D + a_0, \quad \mu_1(s_1^{\text{in}}, s_2^{\text{in}}) < D + a_1 \quad \text{and} \quad \mu_2(s_2^{\text{in}}) < D + a_2.$$

These conditions are equivalent to the conditions of [26], section C1, given in terms of variables (H.1) and growth functions (H.3).

SS2 = $(0, 0, x_2, s_0, s_1, s_2)$ is given by:

$$(G.4) \quad s_0 = s_0^{\text{in}}, \quad s_1 = s_1^{\text{in}}, \quad s_2 = \frac{K_2(D+a_2)}{m_2-D-a_2}, \quad x_2 = \frac{D}{D+a_2} (s_2^{\text{in}} - s_2).$$

It exists if and only if $s_2^{\text{in}} > s_2$, where s_2 is given by (G.4). It is stable if and only if

$$\mu_0(s_0^{\text{in}}, s_2) < D + a_0 \quad \text{and} \quad \mu_1(s_1^{\text{in}}, s_2) < D + a_1.$$

Formulas (G.4) together with the conditions of existence and stability of SS2 were established in [26], section C2, using variables (H.1) and growth functions (H.3).

SS3 = $(x_0, 0, 0, s_0, s_1, s_2)$ is given by:

$$(G.5) \quad x_0 = \frac{D}{D+a_0} (s_0^{\text{in}} - s_0), \quad s_1 = s_1^{\text{in}} + s_0^{\text{in}} - s_0, \quad s_2 = s_2^{\text{in}} - \omega (s_0^{\text{in}} - s_0),$$

where s_0 is a solution of equation

$$(G.6) \quad \frac{m_0 s_0 (s_2^{\text{in}} - \omega (s_0^{\text{in}} - s_0))}{(K_0 + s_0)(L_0 + s_2^{\text{in}} - \omega (s_0^{\text{in}} - s_0))} = D + a_0.$$

Notice that (G.6) is a quadratic equation. Only its solution in the interval

$$J_0 = [\max(0, s_0^{\text{in}} - s_2^{\text{in}}/\omega), s_0^{\text{in}}]$$

is to be considered. SS3 exists if and only if the following condition holds

$$(G.7) \quad \mu_0(s_0^{\text{in}}, s_2^{\text{in}}) > D + a_0.$$

It is stable if and only if

$$(G.8) \quad \begin{aligned} \mu_1(s_0^{\text{in}} - s_0 + s_1^{\text{in}}, s_2^{\text{in}} - \omega (s_0^{\text{in}} - s_0)) &< D + a_1, \\ s_2^{\text{in}} - \omega s_0^{\text{in}} &< M_2(D + a_2) - \omega M_0(D + a_0, M_2(D + a_2)), \end{aligned}$$

where s_0 is the solution in the interval J_0 of equation (G.6). Formulas (G.5) together with equation (G.6) giving s_0 and the stability condition (G.8) were established in [26], section C3, using variables (H.1) and growth functions (H.3). However, neither condition (G.7) of existence of SS3 nor the signs of other eigenvalues of the Jacobian

665 matrix were explicitly established in [26], section C3, where the existence and stabil-
 666 ity of SS3 were checked only numerically by considering the roots of polynomials of
 667 degrees 2 and 3, respectively, see formulas (C.3) and (C.7) in [26].

668 SS4 = $(x_0, x_1, 0, s_0, s_1, s_2)$ is given by:

$$669 \quad (G.9) \quad \begin{aligned} s_0 &= \frac{(D+a_0)K_0(L_0+s_2)}{m_0s_2-(D+a_0)(L_0+s_2)}, & s_1 &= \frac{(D+a_1)K_1(K_I+s_2)}{m_1K_I-(D+a_1)(K_I+s_2)}, \\ 670 \quad x_0 &= \frac{D}{D+a_0} (s_0^{\text{in}} - s_0), & x_1 &= \frac{D}{D+a_1} (s_0^{\text{in}} - s_0 + s_1^{\text{in}} - s_1), \end{aligned}$$

671 where s_2 is a solution of equation

$$672 \quad (G.10) \quad \begin{aligned} (1-\omega) \frac{(D+a_0)K_0(L_0+s_2)}{m_0s_2-(D+a_0)(L_0+s_2)} + \frac{(D+a_1)K_1(K_I+s_2)}{m_1K_I-(D+a_1)(K_I+s_2)} + s_2 \\ 673 \quad = (1-\omega)s_0^{\text{in}} + s_1^{\text{in}} + s_2^{\text{in}}. \end{aligned}$$

674 Notice that (G.10) reduces to a cubic equation in s_2 . Only its solutions in the interval
 675 (s_2^0, s_2^1) are to be considered. The steady states SS4¹ and SS4² exist if and only if the
 676 following conditions hold

$$677 \quad (G.11) \quad s_0^{\text{in}} > s_0, \quad s_0^{\text{in}} + s_1^{\text{in}} > s_0 + s_1 \quad \text{and} \quad (1-\omega)s_0^{\text{in}} + s_1^{\text{in}} + s_2^{\text{in}} \geq \phi_1(D),$$

679 where s_0 and s_1 are defined by (G.9). SS4¹ is unstable whenever it exists and SS4²
 680 is stable if and only if

$$681 \quad (G.12) \quad (1-\omega)s_0^{\text{in}} + s_1^{\text{in}} + s_2^{\text{in}} < \phi_2(D), \quad \text{and} \quad \phi_3(D) > 0.$$

683 Here ϕ_2 and ϕ_3 are defined in Table 8. Formulas (G.9) together with equation (G.10)
 684 giving s_2 were established in [26], section C4, using variables (H.1) and growth func-
 685 tions (H.3). However, neither condition (G.11) of existence of SS4 nor its condition
 686 of stability (G.12) have been established explicitly in [26], section C4, where the exis-
 687 tence and stability of SS4 were checked only numerically by considering the roots of
 688 a polynomial of degree 5, see formula (C.20) in [26].

689 SS5 = $(x_0, 0, x_2, s_0, s_1, s_2)$ is given by:

$$690 \quad (G.13) \quad \begin{aligned} s_2 &= \frac{(D+a_2)K_2}{m_2-D-a_2}, & s_0 &= \frac{(D+a_0)K_0(L_0+s_2)}{m_0s_2-(D+a_0)(L_0+s_2)}, & s_1 &= s_0^{\text{in}} - s_0 + s_1^{\text{in}}, \\ 691 \quad x_0 &= \frac{D}{D+a_0} (s_0^{\text{in}} - s_0), & x_2 &= \frac{D}{D+a_2} (s_2^{\text{in}} - s_2 - \omega (s_0^{\text{in}} - s_0)). \end{aligned}$$

692 It exists if and only if the following conditions hold

$$693 \quad (G.14) \quad s_0^{\text{in}} > s_0, \quad s_2^{\text{in}} - \omega s_0^{\text{in}} > s_2 - \omega s_0.$$

695 where s_0 and s_2 are given by (G.13). SS5 is stable if and only if

$$696 \quad (G.15) \quad s_0^{\text{in}} + s_1^{\text{in}} < M_0(D+a_0, M_2(D+a_2)) + M_1(D+a_1, M_2(D+a_2)).$$

698 Formulas (G.13) together with conditions (G.14) of existence and (G.15) of stability
 699 of SS5 were established in [26], section C5, using variables (H.1) and growth func-
 700 tions (H.3). However, the signs of other eigenvalues of the Jacobian matrix have been
 701 checked only numerically by considering the roots of a polynomial of degree 4, see
 702 formula (C.31) in [26].

703 SS6 = $(x_0, x_1, x_2, s_0, s_1, s_2)$ is given by:

$$704 \quad (G.16) \quad \begin{aligned} s_2 &= \frac{(D+a_2)K_2}{m_2-D-a_2}, & s_0 &= \frac{(D+a_0)K_0(L_0+s_2)}{m_0s_2-(D+a_0)(L_0+s_2)}, & s_1 &= \frac{(D+a_1)K_1(K_I+s_2)}{m_1K_I-(D+a_1)(K_I+s_2)}, \\ x_0 &= \frac{D}{D+a_0} (s_0^{\text{in}} - s_0), & x_1 &= \frac{D}{D+a_1} (s_0^{\text{in}} - s_0 + s_1^{\text{in}} - s_1), \\ 705 \quad x_2 &= \frac{D}{D+a_2} ((1-\omega)(s_0^{\text{in}} - s_0) + s_1^{\text{in}} - s_1 + s_2^{\text{in}} - s_2). \end{aligned}$$

706 It exists if and only if the following conditions hold

$$707 \quad (G.17) \quad s_0^{\text{in}} > s_0, \quad s_0^{\text{in}} + s_1^{\text{in}} > s_0 + s_1, \quad (1 - \omega)s_0^{\text{in}} + s_1^{\text{in}} + s_2^{\text{in}} > \phi_2(D),$$

709 where s_0 and s_1 are given by (G.16). SS6 is stable if and only if

$$710 \quad (G.18) \quad c_i > 0, \quad i = 3, 5, \quad \text{and} \quad r_j > 0, \quad j = 4, 5,$$

712 where c_i and r_j are defined in Table 2. Formulas (G.16) together with conditions
713 (G.17) of existence of SS6 were established in [26], section C6, using variables (H.1)
714 and growth functions (H.3). However, the Liénard-Chipart stability conditions (G.18)
715 were not considered in [26], where the stability of SS6 was checked only numerically
716 by considering the roots of a polynomial of degree 6, see formula (C.42) in [26].

717 SS7 = $(0, x_1, 0, s_0, s_1, s_2)$ is given by:

$$718 \quad (G.19) \quad s_0 = s_0^{\text{in}}, \quad x_1 = \frac{D}{D+a_1} (s_1^{\text{in}} - s_1), \quad s_2 = s_1^{\text{in}} - s_1 + s_2^{\text{in}},$$

720 where s_1 is a unique solution of equation

$$721 \quad (G.20) \quad \frac{m_1 s_1 K_I}{(K_1 + s_1)(K_I + s_1^{\text{in}} + s_2^{\text{in}} - s_1)} = D + a_1.$$

Notice that (G.20) is a quadratic equation. Only its solution in the interval

$$J_1 = [0, s_1^{\text{in}})$$

723 is to be considered. SS7 exists if and only if the following condition holds

$$724 \quad (G.21) \quad \mu_1 (s_1^{\text{in}}, s_2^{\text{in}}) > D + a_1.$$

726 SS7 is stable if and only if

$$727 \quad (G.22) \quad \begin{aligned} s_1^{\text{in}} + s_2^{\text{in}} &< M_1 (D + a_1, M_3 (s_0^{\text{in}}, D + a_0)) + M_3 (s_0^{\text{in}}, D + a_0), \\ s_1^{\text{in}} + s_2^{\text{in}} &< M_1 (D + a_1, M_2 (D + a_2)) + M_2 (D + a_2). \end{aligned}$$

729 Formulas (G.19) together with equation (G.20) giving s_1 and stability condition
730 (G.22) were established in [26], section C7, using variables (H.1) and growth functions
731 (H.3). However, condition (G.21) of existence of SS7 has not been established explic-
732 itly in [26], section C7, where the existence of SS7 and the signs of other eigenvalues
733 of the Jacobian matrix were checked only numerically by considering the roots of a
734 polynomial of degree 3, see formula (C.53) in [26].

735 SS8 = $(0, x_1, x_2, s_0, s_1, s_2)$ is given by:

$$736 \quad (G.23) \quad \begin{aligned} s_0 &= s_0^{\text{in}}, \quad s_2 = \frac{(D+a_2)K_2}{m_2 - D - a_2}, \quad s_1 = \frac{(D+a_1)K_1(K_I + s_2)}{m_1 K_I - (D+a_1)(K_I + s_2)}, \\ 737 \quad x_1 &= \frac{D}{D+a_1} (s_1^{\text{in}} - s_1), \quad x_2 = \frac{D}{D+a_2} (s_1^{\text{in}} - s_1 + s_2^{\text{in}} - s_2). \end{aligned}$$

738 It exists if and only if the following conditions hold

$$739 \quad (G.24) \quad s_1^{\text{in}} > s_1, \quad s_1^{\text{in}} + s_2^{\text{in}} > s_1 + s_2,$$

741 where s_1 and s_2 are given by (G.23). SS8 is stable if and only if

$$742 \quad (G.25) \quad s_0^{\text{in}} < M_0 (D + a_0, M_2 (D + a_2)).$$

744 Formulas (G.23) together with conditions (G.24) of existence and (G.25) of stability
 745 of SS8 were established in [26], section C8, using variables (H.1) and growth functions
 746 (H.3). However, the signs of other eigenvalues of the Jacobian matrix have been
 747 checked only numerically by considering the roots of a polynomial of degree 4, see
 748 formula (C.62) in [26].

749 **Appendix H. Numerical simulations.** The plots of Figures F.1 to F.4 were
 750 performed with Maple [11], which is used in particular for the computations of coeffi-
 751 cients c_3 , c_5 , r_4 and r_5 , evaluated at SS6, and the computations of the eigenvalues of
 752 the Jacobian matrix evaluated at SS6. The plots of Figures E.1 to E.3 were performed
 753 with Scilab [22] by using the formulas of the steady state components given in Table 1.
 754 The various functions appearing in these formulas are given in Table 16. The plots
 755 of Figures 4.2 to 4.4 and H.1 to H.4 were performed with Scilab [22]. The numerical
 756 simulations presented in Figures 4.2 to 4.4, F.4, and H.1 to H.4 were performed on
 757 the dimensionless form of (4.2) used in [26]. Indeed, in the original form (4.2), nu-
 758 merical instabilities arise in numerical schemes. To reduce the number of parameters
 759 describing the dynamics and facilitate numerical simulations, the following rescaling
 760 of the variables was used in [26]:

$$(H.1) \quad \begin{aligned} X_0 &= \frac{X_{ch}}{K_{S,ch}Y_{ch}}, & X_1 &= \frac{X_{ph}}{K_{S,ph}Y_{ph}}, & X_2 &= \frac{X_{H_2}}{K_{S,H_2}Y_{H_2}}, \\ S_0 &= \frac{S_{ch}}{K_{S,ch}}, & S_1 &= \frac{S_{ph}}{K_{S,ph}}, & S_2 &= \frac{S_{H_2}}{K_{S,H_2}}, & \tau &= k_{m,ch}Y_{ch}t. \end{aligned}$$

763 Then, with these changes of variables the system given in (4.2) reduced to system

$$(H.2) \quad \begin{cases} \frac{dX_0}{d\tau} = (\nu_0(S_0, S_2) - \alpha - k_0)X_0 \\ \frac{dX_1}{d\tau} = (\nu_1(S_1, S_2) - \alpha - k_1)X_1 \\ \frac{dX_2}{d\tau} = (\nu_2(S_2) - \alpha - k_2)X_2 \\ \frac{dS_0}{d\tau} = \alpha(u_0 - S_0) - \nu_0(S_0, S_2)X_0 \\ \frac{dS_1}{d\tau} = \alpha(u_1 - S_1) + \omega_0\nu_0(S_0, S_2)X_0 - \nu_1(S_1, S_2)X_1 \\ \frac{dS_2}{d\tau} = \alpha(u_2 - S_2) - \omega_2\nu_0(S_0, S_2)X_0 + \omega_1\nu_1(S_1, S_2)X_1 - \nu_2(S_2)X_2. \end{cases}$$

The operating parameters are

$$\alpha = \frac{D}{k_{m,ch}Y_{ch}}, \quad u_0 = \frac{S_{ch}^{in}}{K_{S,ch}}, \quad u_1 = \frac{S_{ph}^{in}}{K_{S,ph}}, \quad u_2 = \frac{S_{H_2}^{in}}{K_{S,H_2}}.$$

The yield coefficients are

$$\omega_0 = \frac{K_{S,ch}}{K_{S,ph}} \frac{224}{208} (1 - Y_{ch}), \quad \omega_1 = \frac{K_{S,ph}}{K_{S,H_2}} \frac{32}{224} (1 - Y_{ph}), \quad \omega_2 = \frac{16}{208} \frac{K_{S,ch}}{K_{S,H_2}}.$$

The death rates are

$$k_0 = \frac{k_{dec,ch}}{k_{m,ch}Y_{ch}}, \quad k_1 = \frac{k_{dec,ph}}{k_{m,ch}Y_{ch}}, \quad k_2 = \frac{k_{dec,H_2}}{k_{m,ch}Y_{ch}}.$$

766 The growth functions are

$$(H.3) \quad \nu_0(S_0, S_2) = \frac{S_0}{1+S_0} \frac{S_2}{K_P+S_2}, \quad \nu_1(S_1, S_2) = \frac{\phi_1 S_1}{1+S_1} \frac{1}{1+K_I S_2}, \quad \nu_2(S_2) = \frac{\phi_2 S_2}{1+S_2},$$

where the biological parameters are given by

$$\phi_1 = \frac{k_{m,ph}Y_{ph}}{k_{m,ch}Y_{ch}}, \quad \phi_2 = \frac{k_{m,H_2}Y_{H_2}}{k_{m,ch}Y_{ch}}, \quad K_P = \frac{K_{S,H_2,C}}{K_{S,H_2}}, \quad K_I = \frac{K_{S,H_2}}{K_{I,H_2}}.$$

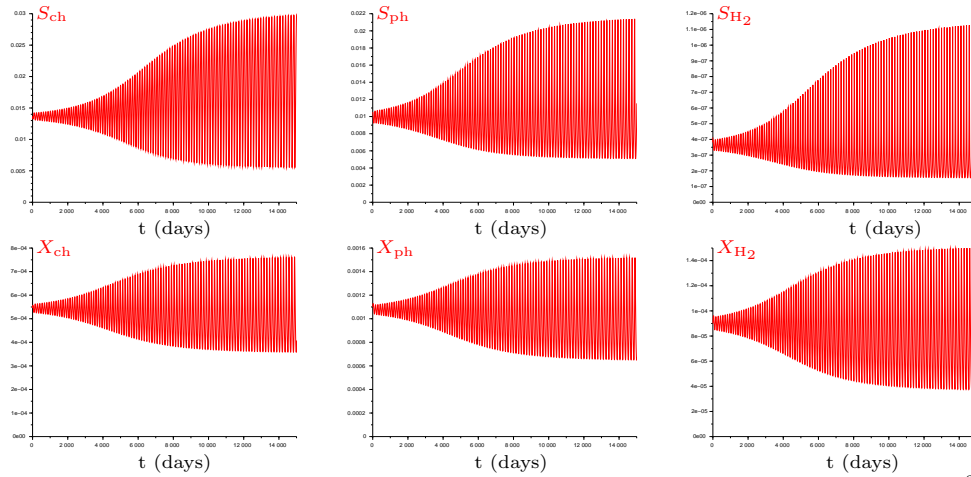


FIG. H.1. Trajectories of S_{ch} , S_{ph} , S_{H_2} , X_{ch} , X_{ph} and X_{H_2} for $S_{ch,in} = 0.0995$ (in kgCOD/m^3): Convergence to the stable limit cycle.

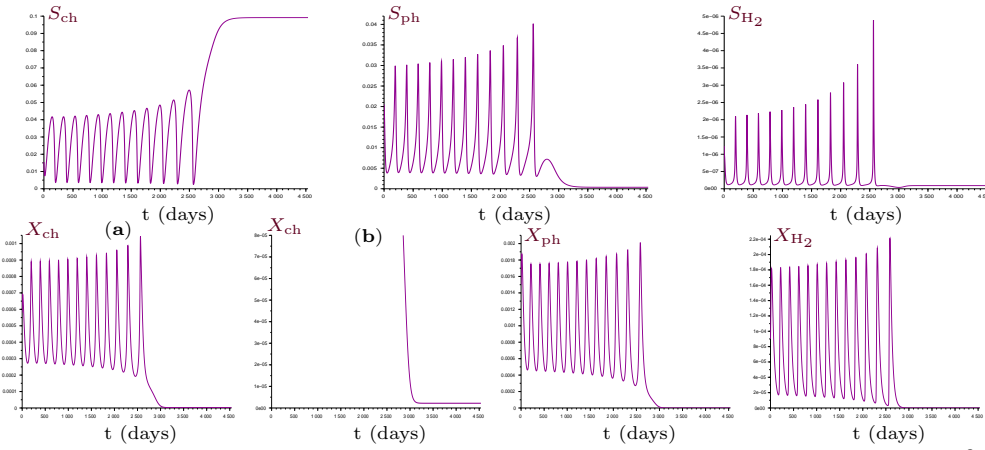


FIG. H.2. Trajectories of S_{ch} , S_{ph} , S_{H_2} , X_{ch} , X_{ph} and X_{H_2} for $S_{ch,in} = 0.0995$ (in kgCOD/m^3): Convergence to the stable steady state SS3. (b) A magnification of (a) showing that the solution of (4.2) converges to the nonzero X_{ch} -component of SS3.

769 The trajectories in Figures 4.2 to 4.4 and H.1 to H.4 were presented according
 770 to the variables of model (4.2) using the change of variables (H.1). In Figures 4.2
 771 to 4.4, the projections of the orbits of the six-dimensional phase space into the three-
 772 dimensional space $(X_{ch}, X_{ph}, X_{H_2})$ shows the appearance and disappearance of a sta-
 773 ble limit cycle for different values of $S_{ch}^{in} > \sigma_5$. The plot of the limit cycle was obtained
 774 by solving the ordinary differential equations using the default solver “*lsoda*” from the
 775 ODEPACK package in Scilab. Tables 13 and 14 present the components of the stable
 776 steady states SS3 and SS6, and all the initial conditions chosen to trace the different
 777 trajectories of model (4.2) in Figures 4.2 to 4.4 and H.1 to H.4.

778 **Appendix I. Tables.** In this section, the biological parameter values are
 779 provided in Table 15. In Table 16, we present the auxiliary functions in the case of
 780 the growth functions given by (G.3).

781 **Acknowledgments.** The authors thank the Editor and the two anonymous
 782 reviewers for their constructive comments which have greatly improved this work.

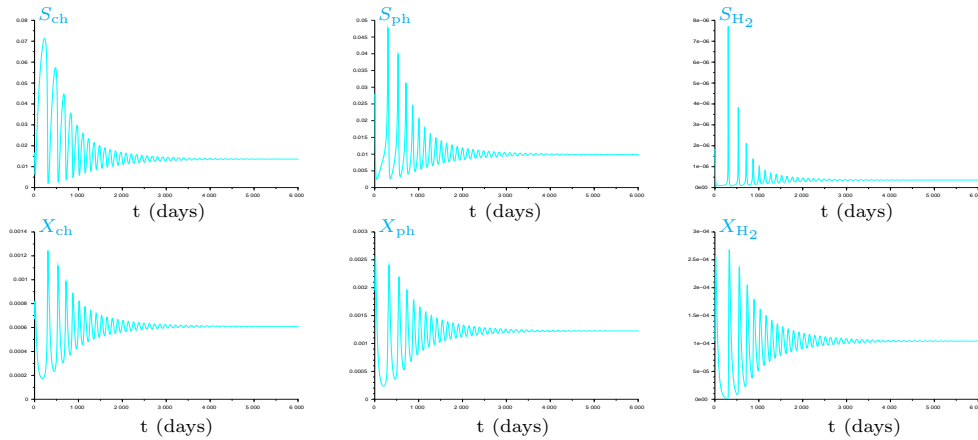


FIG. H.3. Trajectories of S_{ch} , S_{ph} , S_{H_2} , X_{ch} , X_{ph} and X_{H_2} for $S_{ch,in} = 0.11$ (in kgCOD/m^3): Convergence to the positive steady state SS6.

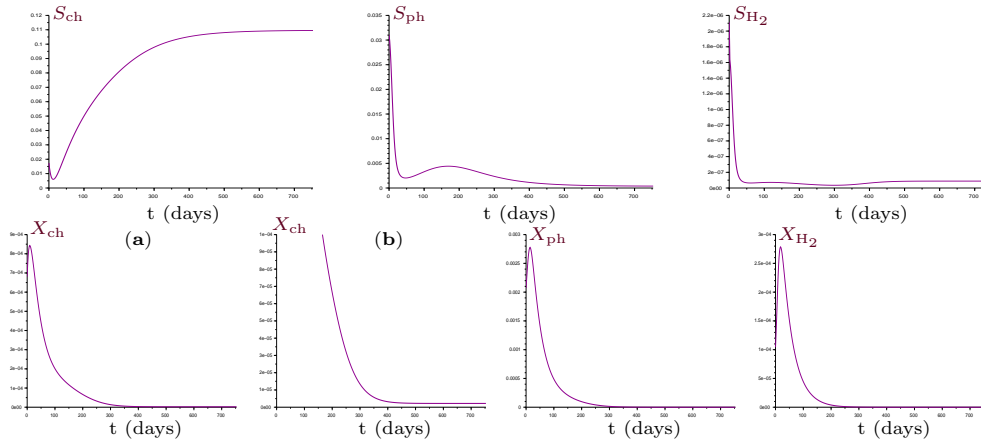


FIG. H.4. Trajectories of S_{ch} , S_{ph} , S_{H_2} , X_{ch} , X_{ph} and X_{H_2} for $S_{ch,in} = 0.11$ (in kgCOD/m^3): Convergence to the stable steady state SS3. (b) A magnification of (a) showing that the solution of (4.2) converges to the nonzero X_{ch} -component of SS3.

783

REFERENCES

784 [1] D. Batstone, J. Keller, I. Angelidaki, S. Kalyuzhnyi, S. Pavlostathis, A. Rozzi, W. Sanders,
 785 H. Siegrist, and V. Vavilin, *The IWA Anaerobic Digestion Model No 1 (ADM1)*, Water
 786 Sci Technol., 45 (2002), pp. 65–73, <https://doi.org/10.2166/wst.2002.0292>.
 787 [2] B. Benyahia, T. Sari, B. Cherki, and J. Harmand, *Bifurcation and stability analysis of a two step*
 788 *model for monitoring anaerobic digestion processes*, J. Proc. Control, 22 (2012), pp. 1008–
 789 1019, <https://doi.org/10.1016/j.jprocont.2012.04.012>.
 790 [3] O. Bernard, Z. Hadj-Sadok, D. Dochain, A. Genovesi, and J.-P. Steyer, *Dynamical model develop-*
 791 *ment and parameter identification for an anaerobic wastewater treatment process*, Biotechnol.
 792 Bioeng., 75 (2001), pp. 424–438, <https://doi.org/10.1002/bit.10036>.
 793 [4] A. Bornhöft, R. Hanke-Rauschenbach, and K. Sundmacher, *Steady-state analysis of the Anaerobic*
 794 *Digestion Model No. 1 (ADM1)*, J. Nonlinear Dyn., 73 (2013), pp. 535–549, [https://doi.](https://doi.org/10.1007/s11071-013-0807-x)
 795 [org/10.1007/s11071-013-0807-x](https://doi.org/10.1007/s11071-013-0807-x).
 796 [5] A. Burchard, *Substrate degradation by a mutualistic association of two species in the chemostat*,
 797 J. Math. Biol., 32 (1994), pp. 465–489, <https://doi.org/10.1007/BF00160169>.
 798 [6] W. A. Coppel, *Stability and Asymptotic Behavior of Differential Equations*, D.C. Heath, Boston,
 799 1965.

TABLE 13

Steady states SS3 and SS6 of model (4.2) corresponding to Figures 4.2 to 4.4 and H.1 to H.4. The biological parameters are provided in Table 15. The operating parameters are $D = 0.01$, $S_{\text{ph}}^{\text{in}} = 0$, $S_{\text{H}_2}^{\text{in}} = 2.67 \times 10^{-5}$ and $S_{\text{ch}}^{\text{in}}$ given in the second column.

Figure	$S_{\text{ch}}^{\text{in}}$	SS3 = $(X_{\text{ch}}, 0, 0, S_{\text{ch}}, S_{\text{ph}}, S_{\text{H}_2})$ SS6 = $(X_{\text{ch}}, X_{\text{ph}}, X_{\text{H}_2}, S_{\text{ch}}, S_{\text{ph}}, S_{\text{H}_2})$
4.2	0.098	$(2.19 \cdot 10^{-6}, 0, 0, 9.77 \cdot 10^{-2}, 3.65 \cdot 10^{-4}, 9.17 \cdot 10^{-8})$ $(5.34 \cdot 10^{-4}, 1.06 \cdot 10^{-3}, 8.80 \cdot 10^{-5}, 1.36 \cdot 10^{-2}, 9.93 \cdot 10^{-3}, 3.62 \cdot 10^{-7})$
4.3	0.0995	$(2.19 \cdot 10^{-6}, 0, 0, 9.92 \cdot 10^{-2}, 3.65 \cdot 10^{-4}, 9.12 \cdot 10^{-8})$
H.1 H.2		$(5.44 \cdot 10^{-4}, 1.08 \cdot 10^{-3}, 9.00 \cdot 10^{-5}, 1.36 \cdot 10^{-2}, 9.93 \cdot 10^{-3}, 3.62 \cdot 10^{-7})$
4.4	0.11	$(2.19 \cdot 10^{-6}, 0, 0, 1.10 \cdot 10^{-1}, 3.65 \cdot 10^{-4}, 8.79 \cdot 10^{-8})$
H.3		$(6.10 \cdot 10^{-4}, 1.22 \cdot 10^{-3}, 1.04 \cdot 10^{-4}, 1.36 \cdot 10^{-2}, 9.93 \cdot 10^{-3}, 3.62 \cdot 10^{-7})$
H.4		

TABLE 14

The initial conditions of solutions of model (4.2) in Figures 4.2 to 4.4 and H.1 to H.4 are obtained from the initial conditions of the solutions of model (H.2) by using the change of variables (H.1). The initial conditions of (H.2) are given by $X_i(0) = X_i^* + \varepsilon$ and $S_i(0) = S_i^* + \varepsilon$, $i = 0, 1, 2$ where X_i^* and S_i^* are the components of SS6 and ε is given in the second column. When there is more than one trajectory in the figure, its color is indicated in the first column.

Figure Color	ε	$(X_{\text{ch}}(0), X_{\text{ph}}(0), X_{\text{H}_2}(0), S_{\text{ch}}(0), S_{\text{ph}}(0), S_{\text{H}_2}(0))$
4.2	$9.7 \cdot 10^{-3}$	$(5.44 \cdot 10^{-4}, 1.17 \cdot 10^{-3}, 8.80 \cdot 10^{-5}, 1.42 \cdot 10^{-2}, 1.29 \cdot 10^{-2}, 6.05 \cdot 10^{-7})$
4.3		
Pink	10^{-2}	$(5.54 \cdot 10^{-4}, 1.20 \cdot 10^{-3}, 9.00 \cdot 10^{-5}, 1.42 \cdot 10^{-2}, 1.29 \cdot 10^{-2}, 6.12 \cdot 10^{-7})$
Blue	$3.2 \cdot 10^{-2}$	$(5.76 \cdot 10^{-4}, 1.46 \cdot 10^{-3}, 9.00 \cdot 10^{-5}, 1.53 \cdot 10^{-2}, 1.96 \cdot 10^{-2}, 1.16 \cdot 10^{-6})$
Green	$3.5 \cdot 10^{-2}$	$(5.79 \cdot 10^{-4}, 1.50 \cdot 10^{-3}, 9.00 \cdot 10^{-5}, 1.55 \cdot 10^{-2}, 2.05 \cdot 10^{-2}, 1.24 \cdot 10^{-6})$
4.4		
Blue	$6 \cdot 10^{-2}$	$(6.71 \cdot 10^{-4}, 1.95 \cdot 10^{-3}, 1.04 \cdot 10^{-4}, 1.68 \cdot 10^{-2}, 2.80 \cdot 10^{-2}, 1.86 \cdot 10^{-6})$
Green	$7 \cdot 10^{-2}$	$(6.81 \cdot 10^{-4}, 2.07 \cdot 10^{-3}, 1.04 \cdot 10^{-4}, 1.74 \cdot 10^{-2}, 3.11 \cdot 10^{-2}, 2.11 \cdot 10^{-6})$
H.1	$2 \cdot 10^{-3}$	$(5.46 \cdot 10^{-4}, 1.10 \cdot 10^{-3}, 9.00 \cdot 10^{-5}, 1.37 \cdot 10^{-2}, 1.05 \cdot 10^{-2}, 4.12 \cdot 10^{-7})$
H.2	$3.5 \cdot 10^{-2}$	$(5.79 \cdot 10^{-4}, 1.50 \cdot 10^{-3}, 9.00 \cdot 10^{-5}, 1.55 \cdot 10^{-2}, 2.05 \cdot 10^{-2}, 1.24 \cdot 10^{-6})$
H.3	$6 \cdot 10^{-2}$	$(6.71 \cdot 10^{-4}, 1.95 \cdot 10^{-3}, 1.04 \cdot 10^{-4}, 1.68 \cdot 10^{-2}, 2.80 \cdot 10^{-2}, 1.86 \cdot 10^{-6})$
H.4	$7 \cdot 10^{-2}$	$(6.81 \cdot 10^{-4}, 2.07 \cdot 10^{-3}, 1.04 \cdot 10^{-4}, 1.74 \cdot 10^{-2}, 3.11 \cdot 10^{-2}, 2.11 \cdot 10^{-6})$

- 800 [7] Y. Daoud, N. Abdellatif, T. Sari, and J. Harmand, *Steady state analysis of a syntrophic model:*
801 *The effect of a new input substrate concentration*, Math. Model. Nat. Phenom., 13 (2018),
802 pp. 1–22, <https://doi.org/10.1051/mmnp/2018037>.
- 803 [8] M. El Hajji, N. Chorfi, and M. Jleli, *Mathematical modelling and analysis for a three-tiered*
804 *microbial food web in a chemostat*, Electron. J. Differ. Equ., 255 (2017), pp. 1–13.
- 805 [9] M. El Hajji, F. Mazenc, and J. Harmand, *A mathematical study of a syntrophic relationship*
806 *of a model of anaerobic digestion process*, Math. Biosci. Eng., 7 (2010), pp. 641–656,
807 <https://doi.org/10.3934/mbe.2010.7.641>.
- 808 [10] F. Gantmacher, *Application of the theory of matrices*, Interscience Publishers, INC. New York,
809 2004.
- 810 [11] MAPLE, *version 17.0.0.0*, Waterloo Maple Inc., Waterloo, Ontario, 2018.
- 811 [12] C. Martinez, A. Ávila, F. Mairet, L. Meier, and D. Jeison, *Modeling and analysis of an absorption*
812 *column connected to a microalgae culture*, SIAM J. Appl. Math., 80 (2020), pp. 772–791,
813 <https://doi.org/10.1137/18M1225641>.
- 814 [13] J. Mata-Alvarez, S. Macè, and P. Llabrès, *Anaerobic digestion of organic solid wastes. an overview*
815 *of research achievements and perspectives*, Bioresour. Technol., 74 (2000), pp. 3–16, [https://doi.org/10.1016/S0960-8596\(00\)00003-9](https://doi.org/10.1016/S0960-8596(00)00003-9).

TABLE 15

Nominal parameter values, where $i = \text{ch, ph, H}_2$. Units are expressed in Chemical Oxygen Demand (COD).

Parameters	Nominal values	Units
$k_{m,\text{ch}}$	29	kgCOD _S /kgCOD _X /d
$K_{S,\text{ch}}$	0.053	kgCOD/m ³
Y_{ch}	0.019	kgCOD _X /kgCOD _S
$k_{m,\text{ph}}$	26	kgCOD _S /kgCOD _X /d
$K_{S,\text{ph}}$	0.302	kgCOD/m ³
Y_{ph}	0.04	kgCOD _X /kgCOD _S
k_{m,H_2}	35	kgCOD _S /kgCOD _X /d
K_{S,H_2}	2.5×10 ⁻⁵	kgCOD/m ³
$K_{S,\text{H}_2,\text{c}}$	1.0×10 ⁻⁶	kgCOD/m ³
Y_{H_2}	0.06	kgCOD _X /kgCOD _S
$k_{\text{dec},i}$	0.02	d ⁻¹
K_{I,H_2}	3.5×10 ⁻⁶	kgCOD/m ³

TABLE 16

Auxiliary functions in the case of growth functions given by (G.3).

Auxiliary function	Definition domain
$M_0(y, s_2) = \frac{yK_0(L_0+s_2)}{m_0s_2-y(L_0+s_2)}$	$0 \leq y < \frac{m_0s_2}{L_0+s_2}$
$M_1(y, s_2) = \frac{yK_1(K_I+s_2)}{m_1K_I-y(K_I+s_2)}$	$0 \leq y < \frac{m_1K_I}{K_I+s_2}$
$M_2(y) = \frac{yK_2}{m_2-y}$	$0 \leq y < m_2$
$M_3(s_0, z) = \frac{zL_0(K_0+s_0)}{m_0s_0-z(K_0+s_0)}$	$0 \leq z < \frac{m_0s_0}{K_0+s_0}$
$s_2^0(D) = \frac{L_0(D+a_0)}{m_0-D-a_0}$	$D + a_0 < m_0$
$s_2^1(D) = \frac{K_I(m_1-D-a_1)}{D+a_1}$	$D + a_1 < m_1$
$\Psi(s_2, D) = (1 - \omega) \frac{(D+a_0)K_0(L_0+s_2)}{m_0s_2-(D+a_0)(L_0+s_2)} + \frac{(D+a_1)K_1(K_I+s_2)}{m_1K_I-(D+a_1)(K_I+s_2)} + s_2$	$\{D \in I_1 : s_2^0 < s_2 < s_2^1\}$
$\psi_0(s_0) = \frac{m_0s_0(s_2^{\text{in}} - \omega(s_0^{\text{in}} - s_0))}{(K_0+s_0)(L_0+s_2^{\text{in}} - \omega(s_0^{\text{in}} - s_0))}$	$s_0 \in [\max(0, s_0^{\text{in}} - s_2^{\text{in}}/\omega), +\infty)$
$\psi_1(s_1) = \frac{m_1s_1K_I}{(K_1+s_1)(K_I+s_2^{\text{in}}+s_1^{\text{in}}-s_1)}$	$s_1 \in [0, s_1^{\text{in}} + s_2^{\text{in}}]$

816 //doi.org/10.1016/S0960-8524(00)00023-7.
 817 [14] R. May, *Stability and Complexity in Model Ecosystems*, Princeton Univ. Press, NJ., USA, 1973.
 818 [15] T. Meadows, M. Weedermann, and G. Wolkowicz, *Global analysis of a simplified model of anaero-*
 819 *bic digestion and a new result for the chemostat*, SIAM J. Appl. Math., 79 (2019), pp. 668–
 820 689, <https://doi.org/10.1137/18M1198788>.
 821 [16] S. Nouaoura, R. Fekih-Salem, N. Abdellatif, and T. Sari, *Mathematical analysis of a three-tiered*
 822 *food-web in the chemostat*, Discrete & Continuous Dyn. Syst. - B, (2020), [https://doi.org/](https://doi.org/10.3934/dcdsb.2020369)
 823 [10.3934/dcdsb.2020369](https://doi.org/10.3934/dcdsb.2020369).
 824 [17] P. J. Reilly, *Stability of commensalistic systems*, Biotechnol. Bioeng., 16 (1974), pp. 1373–1392,
 825 <https://doi.org/10.1002/bit.260161006>.
 826 [18] T. Sari, M. El Hajji, and J. Harmand, *The mathematical analysis of a syntrophic relationship*
 827 *between two microbial species in a chemostat*, Math. Biosci. Eng., 9 (2012), pp. 627–645,
 828 <https://doi.org/10.3934/mbe.2012.9.627>.
 829 [19] T. Sari and J. Harmand, *A model of a syntrophic relationship between two microbial species in*
 830 *a chemostat including maintenance*, Math. Biosci., 275 (2016), pp. 1–9, [https://doi.org/](https://doi.org/10.1016/j.mbs.2016.02.008)
 831 [10.1016/j.mbs.2016.02.008](https://doi.org/10.1016/j.mbs.2016.02.008).
 832 [20] T. Sari and M. J. Wade, *Generalised approach to modelling a three-tiered microbial food-web*,
 833 Math. Biosci., 291 (2017), pp. 21–37, <https://doi.org/10.1016/j.mbs.2017.07.005>.

- 834 [21] M. Sbarciog, M. Loccufier, and E. Noldus, *Determination of appropriate operating strategies for*
835 *anaerobic digestion systems*, Biochem. Eng. J., 51 (2010), pp. 180–188, [https://doi.org/](https://doi.org/10.1016/j.bej.2010.06.016)
836 [10.1016/j.bej.2010.06.016](https://doi.org/10.1016/j.bej.2010.06.016).
- 837 [22] SCILAB, *version 6.0.1(64-bit)*, Scilab Enterprises SAS, 2018.
- 838 [23] S. Sobieszek, M. J. Wade, and G. S. K. Wolkowicz, *Rich dynamics of a three-tiered anaerobic*
839 *food-web in a chemostat with multiple substrate inflow*, Math. Biosci. Eng., 17 (2020),
840 pp. 7045–7073, <https://doi.org/10.3934/mbe.2020363>.
- 841 [24] E. I. P. Volcke, M. Sbarciog, E. J. L. Noldus, B. De Baets, and M. Loccufier, *Steady state multiplicity*
842 *of two-step biological conversion systems with general kinetics*, Math. Biosci., 228 (2010),
843 pp. 160–170, <https://doi.org/10.1016/j.mbs.2010.09.004>.
- 844 [25] M. Wade, *Not just numbers: Mathematical modelling and its contribution to anaerobic digestion*
845 *processes*, Processes, 8 (2020), p. 888, <https://doi.org/10.3390/pr8080888>.
- 846 [26] M. J. Wade, R. W. Pattinson, N. G. Parker, and J. Doling, *Emergent behaviour in a chlorophenol-*
847 *mineralising three-tiered microbial ‘food web’*, J. Theoret. Biol., 389 (2016), pp. 171–186,
848 <https://doi.org/10.1016/j.jtbi.2015.10.032>.
- 849 [27] M. Weeder mann, G. Seo, and G. S. K. Wolkowicz, *Mathematical model of anaerobic digestion*
850 *in a chemostat: Effects of syntrophy and inhibition*, J. Biol. Dyn., 7 (2013), pp. 59–85,
851 <https://doi.org/10.1080/17513758.2012.755573>.
- 852 [28] M. Weeder mann, G. S. K. Wolkowicz, and J. Sasara, *Optimal biogas production in a model for*
853 *anaerobic digestion*, J. Nonlinear Dyn., 81 (2015), pp. 1097–1112, [https://doi.org/10.1007/](https://doi.org/10.1007/s11071-015-2051-z)
854 [s11071-015-2051-z](https://doi.org/10.1007/s11071-015-2051-z).
- 855 [29] A. Xu, J. Doling, T. P. Curtis, G. Montague, and E. Martin, *Maintenance affects the stability*
856 *of a two-tiered microbial ‘food chain’?*, J. Theoret. Biol., 276 (2011), pp. 35–41, <https://doi.org/10.1016/j.jtbi.2011.01.026>.
857